



# Science & Technology Facilities Council e-Science

SCARF Annual Report 2009-2010

Version : 1.2

Date: 22/12/2010

Edited by Peter Oliver ([peter.oliver@stfc.ac.uk](mailto:peter.oliver@stfc.ac.uk)) 01235 441564

Content written by the respective authors

DATE	REVISION	CHANGES
22/12/10	1.2	Revised after comments by John Gordon
10/11/10	1.1	Added SCARF Changes Appendix
20/10/10	1.0	Initial document

## Abstract

Annual Report on the Usage and Scientific Impact of the SCARF Service

## Dissemination

This is a public document

**Contents**

<b>1.</b>	<b>SCARF Service</b>	<b>3</b>
1.1	SCARF Usage by Department	3
1.2	SCARF Availability	4
1.3	SCARF Developments 2009-10	4
1.4	Future Development	5
1.5	Help and Support	5
<b>2.</b>	<b>Publications and Presentations</b>	<b>5</b>
2.1	Publications	5
2.2	Presentations	5
<b>3.</b>	<b>Science Highlights</b>	<b>5</b>
3.1	<b>Alex Robinson, Raoul Trines &amp; Rob Clark, CLF</b>	<b>5</b>
3.1.1	CLF Plasma Physics SCARF Usage	5
3.2	<b>Timmy Ramirez-Cuesta, ISIS</b>	<b>8</b>
3.2.1	Studying the dynamics of hydrogen using Inelastic Neutron Scattering and Computer Modelling: Neutron Scattering and Hydrogen Storage	8
3.3	<b>Stewart Parker, ISIS</b>	<b>10</b>
3.3.1	Inelastic neutron scattering spectroscopy (INS)	10
3.4	<b>Sanghamitra Mukhopadhyay Imperial College London and STFC</b>	<b>11</b>
3.4.1	Investigation of new generation materials for solid oxide fuel cells (SOFCs).	11
3.4.2	Investigation on Mn doped Silicon for spintronics Applications	12
3.4.3	First principle simulations of AlF <sub>3</sub> surfaces	13
3.5	<b>Mark Quinn, Strathclyde University</b>	<b>13</b>
3.5.1	Ultra-intense laser-solid interactions and fast electron transport in solid density plasma	13
3.6	<b>Stephen Brooks, AsTeC</b>	<b>14</b>
3.6.1	Optimising Pion Production Target Shapes for the Neutrino Factory	14
3.6.2	First Sequence –only removing material	14
3.7	<b>Matthew Krzystyniak, ISIS</b>	<b>15</b>
3.7.1	Software Tools for comparing ab initio calculated proton dynamical features with the results of neutron spectroscopic studies	15
3.8	<b>Keith Refson, CSE</b>	<b>16</b>
3.8.1	Plane-wave Materials Simulation on SCARF with CASTEP	16
3.9	<b>Iain McKenzie, ISIS</b>	<b>17</b>
3.9.1	Muoniated Spin Probes in Soft Matter	17
3.10	<b>Rowan Hargreaves(ISIS), Karen Edler (Bath) and Daniel Bowron (ISIS)</b>	<b>18</b>
3.10.1	Using Empirical Potential Structure Refinement (EPSR) to model n-Decyltrimethylammonium (C10TAB) Bromide micelles	18
3.11	<b>David Royse ISIS</b>	<b>21</b>
3.11.1	Geometry optimisations and phonon calculations	21
3.12	<b>Dean Adams ISIS Accelerator Physics Group</b>	<b>21</b>
3.12.1	Particle Tracking using ORBIT	21
<b>1.</b>	<b>APPENDIX : SCARF Hardware Details</b>	<b>23</b>
<b>2.</b>	<b>APPENDIX: Index of Figures</b>	<b>23</b>
<b>3.</b>	<b>APPENDIX: Publications and Presentations</b>	<b>24</b>
<b>4.</b>	<b>APPENDIX: SCARF Queue Usage 2009-10</b>	<b>30</b>
4.1	General SCARF Queue	30
4.2	SCARF-Lexicon[1-2] Queues	31
4.3	SCARF-IBIS	32
<b>5.</b>	<b>Appendix – SCARF Developments</b>	<b>33</b>
5.1	NGS Software Stack	33
5.2	SCARF Systems Management	33
5.3	People	33

## 1. SCARF SERVICE

SCARF is a High Performance Cluster for STFC staff, Facilities (ISIS, DIAMOND, CLF) and their users. The SCARF Service was started in 2004 and has been upgraded year on year and now represents a significant capital investment in High Performance Computing. Overall SCARF now has over 2000 CPU cores, 5TB memory and 100TB of disk space (Details in Appendix 1). This report covers the year 2009-10 and outlines the research that SCARF has enabled.

### 1.1 SCARF Usage by Department

Each time a researcher uses the SCARF service the CPU time used is recorded. In total over 5.4M CPU hours were used on SCARF during 2009-10.

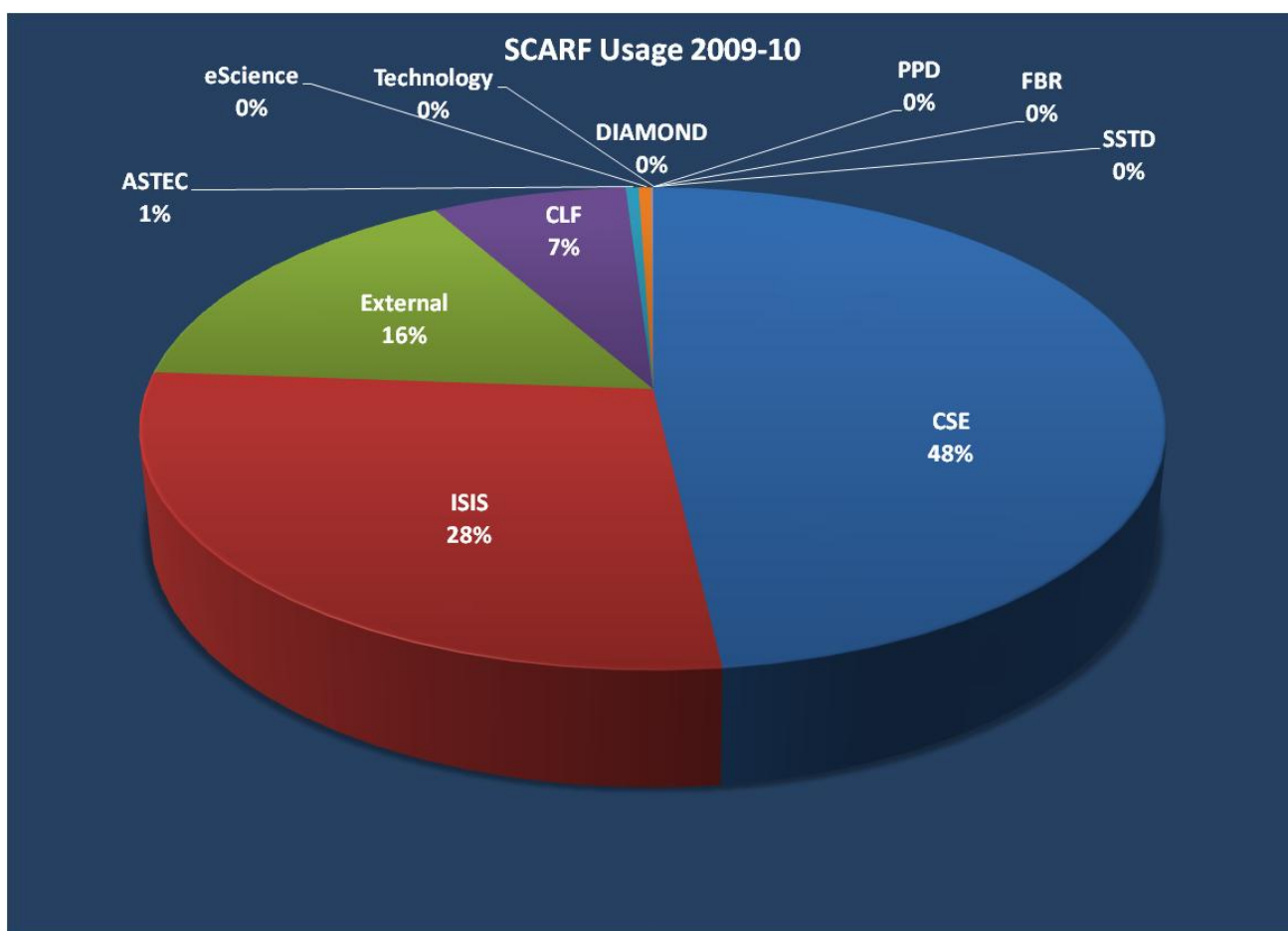


Figure 1 Pie chart showing percentage usage of the SCARF service by department

It is clear from the usage chart that ISIS and CSE are the largest users of SCARF. The External Use category measures the usage from STFC collaborations with Glasgow University, Imperial College, Oxford University and Queens University Belfast.

Section 2 highlights some of the scientific achievements that SCARF has enabled.

### 1.2 SCARF Availability

The availability of SCARF is given in the figure below. This availability measures when users could login to SCARF and submit jobs . SCARF achieved 98.7% availability during 2009-10

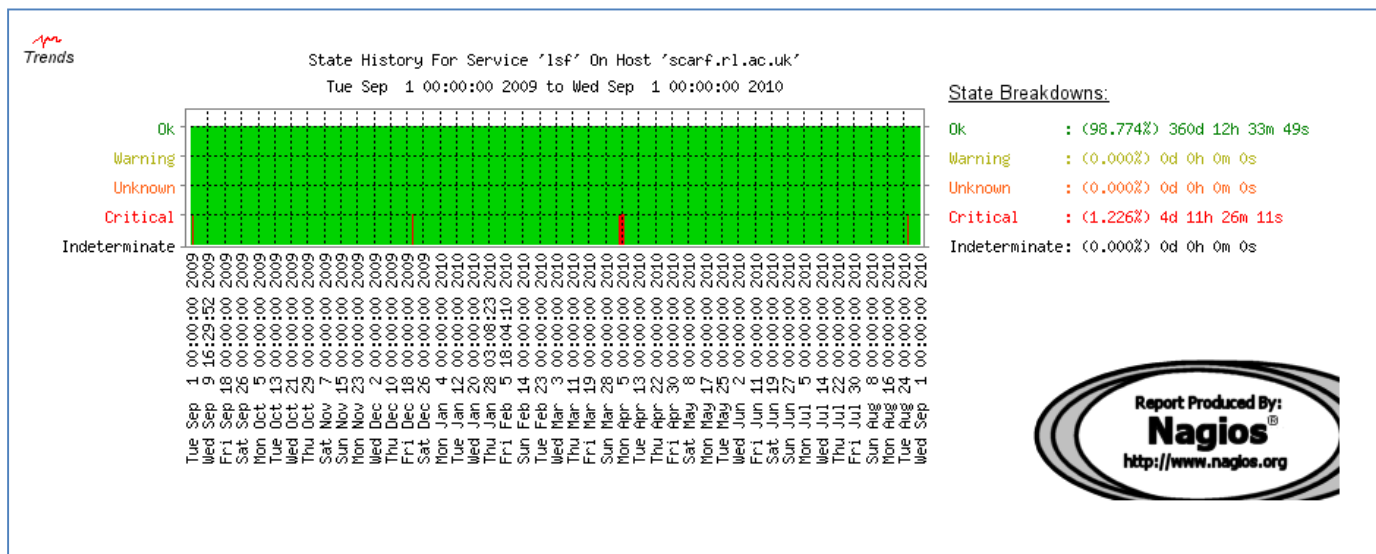


Figure 2: Availability for SCARF

The table below details the availability of compute nodes by purchase date. It is evident that the older equipment purchased in 2006 is giving the most problems. This supports the rolling upgrade of SCARF and the 2006 equipment will be phased out in 2010-11.

Year Purchased	Compute node Availability
2006	94.2%
2007	98.5%
2008	99.2%
2009	98.4%
2010	98.8%

Figure 3: Availability vs Year Purchased

### 1.3 SCARF Developments 2009-10

Major SCARF Developments are listed below. A more detailed list can be found in Appendix 5

- New capacity added
  - 292 Intel E5530 CPU cores for general use
  - 544 Intel E5530 CPU cores for CLF use – SCARF-Lexicon-2
- New applications installed or upgraded
  - G09\_B01
  - Materials Studio Gateway
  - Abaqus 6.8
  - CASTEP 5.5
  - dl\_poly 2.20, 3.10
  - PGI Compiler 10.9
- New Single Sign-on released so users can use their federal id and passwd to access SCARF resources

## 1.4 Future Development

- SCARF 2011 Hardware Upgrade
  - ~384 Intel X5660 CPU Cores for General Use
- SCARF Advisory Board Request
  - Investigations into Advanced Reservation and Co-allocation of Compute and beamline time for ISIS experiment

## 1.5 Help and Support

For any queries concerning the SCARF service please email the SCARF Helpdesk;

[scarf@hpc-support.rl.ac.uk](mailto:scarf@hpc-support.rl.ac.uk)

## 2. PUBLICATIONS AND PRESENTATIONS

### 2.1 Publications

A list of publications is given in Appendix 3. A way of estimating the impact that SCARF has had is to analyse the Journal Impact Factor using the Journal Citation Reports published by Thomson Reuters. The average Impact Factor for Journals published as a result of using SCARF is 4.3 . This compares to an average impact factor across all 6600 journals of 2.2. This is a simplistic analysis but demonstrates that the science done on SCARF is having a significant impact.

The largest impact factor 16.8 is for the Nature Physics Paper:

R. Trines, F. Fiuza, R. Bingham, R. Fonseca, L.O. Silva, A. Cairns and P. Norreys "Simulations of efficient Raman amplification into the multi-Petawatt regime" Nature Physics, PUBLISHED ONLINE: 10 OCTOBER 2010 | DOI: 10.1038/NPHYS1793.

This demonstrates that SCARF produces World Class science.

### 2.2 Presentations

Over 80 presentations are listed in Appendix 3 given all over the world. This demonstrates that SCARF is having a international impact on science around the globe.

## 3. SCIENCE HIGHLIGHTS

### 3.1 Alex Robinson, Raoul Trines & Rob Clark, CLF

#### 3.1.1 CLF Plasma Physics SCARF Usage

The past two years have seen intense activity in a number of areas. This includes work on fast electron transport, Fast Ignition ICF, ion acceleration, short pulse driven hydrodynamics, electron acceleration, and Raman amplification of laser pulses in plasmas. It is difficult to sum up all this work in a few sentences. To illustrate our work we have chosen two examples. The first is a new concept Dr. Robinson has recently developed for Fast Ignition ICF which builds upon his previous theoretical work that used SCARF-LEXICON and experiments done at the CLF. This is illustrated below:

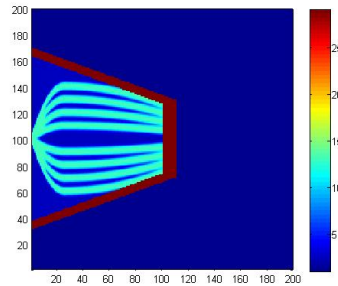


**Figure 4 Slice through the Magnetic Switchyard**

Figure 4 shows an x-y slice through the “Magnetic Switchyard” which is rotationally symmetric and sits inside the standard Cu or Au FI cone. It consists of series of shaped Al shells or petals (cyan regions) which are embedded in plastic. The resistivity gradients at the Al-CH boundaries generate strong magnetic fields all along these boundaries when diverging fast electrons are driven into the switchyard from the left hand boundary. This array acts like a focussing lens which produces a converging beam of fast electrons at the cone tip. Thus we have a device that can turn a diverging fast electron flow into a converging one which is a crucial development for FI.

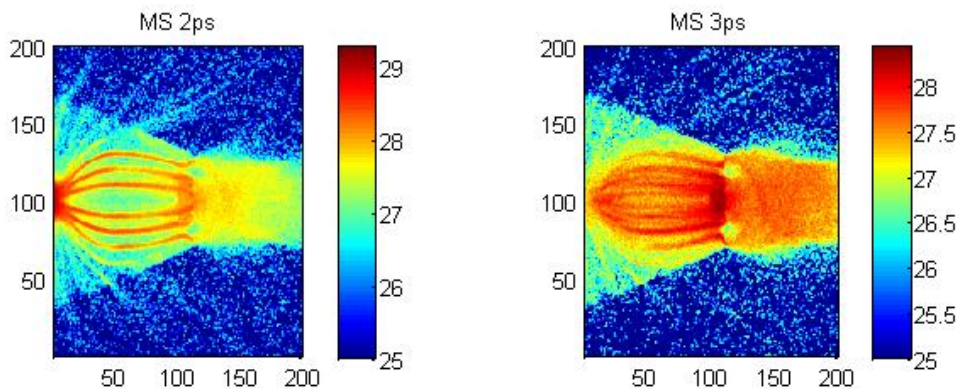


**Figure 5 Fast Electron Flow through Magnetic Switchyard . Fast Electrons enter as hemispherically divergent flow and are focussed into a beam**

The second example is work done by Dr. Trines on Raman amplification in plasmas. Raman amplification is a process by which two counter propagating laser pulses of different frequency interact in plasma, and energy is flowing from the higher frequency pulse to the lower frequency pulse. The higher frequency “pump” pulse is normally around 1000 times longer than the lower frequency “probe” pulse. Once most of the energy of the long pump has been transferred to the short probe, the probe will have a final intensity which is several hundred times that of the pump, hence the term “Raman amplification”. Since the process takes place in plasma, one does not have to worry about “burning” optics, and very high intensities and laser powers can be obtained in a very small (mm-size) volume of plasma.

Since Raman amplification in plasma was first proposed by Malkin, Shvets and Fisch, many researchers have investigated this scheme, but there have been very few attempts to develop the scheme for practical use. In our paper, we present a comprehensive sequence of simulation results, covering many aspects of Raman amplification and identifying the parameter regime where Raman amplification will produce good results. Outside this regime, the growing probe pulse is either destroyed by laser-plasma instabilities, or the energy transfer from pump to probe is inefficient;

these aspects were overlooked by earlier studies. Preserving the smooth envelope of the probe during amplification is important: a smooth probe can be focused very tightly, while a “spiky” probe can only be focused to a much larger spot, leading to a much lower focused intensity. In Figure 6 below, we show the amplification of a probe for favourable and unfavourable parameters; the difference in smoothness between these probes is obvious. The smooth probe has a final power of 2 Petawatt, which is comparable to the peak power of the world’s most powerful solid-state laser systems currently operational.

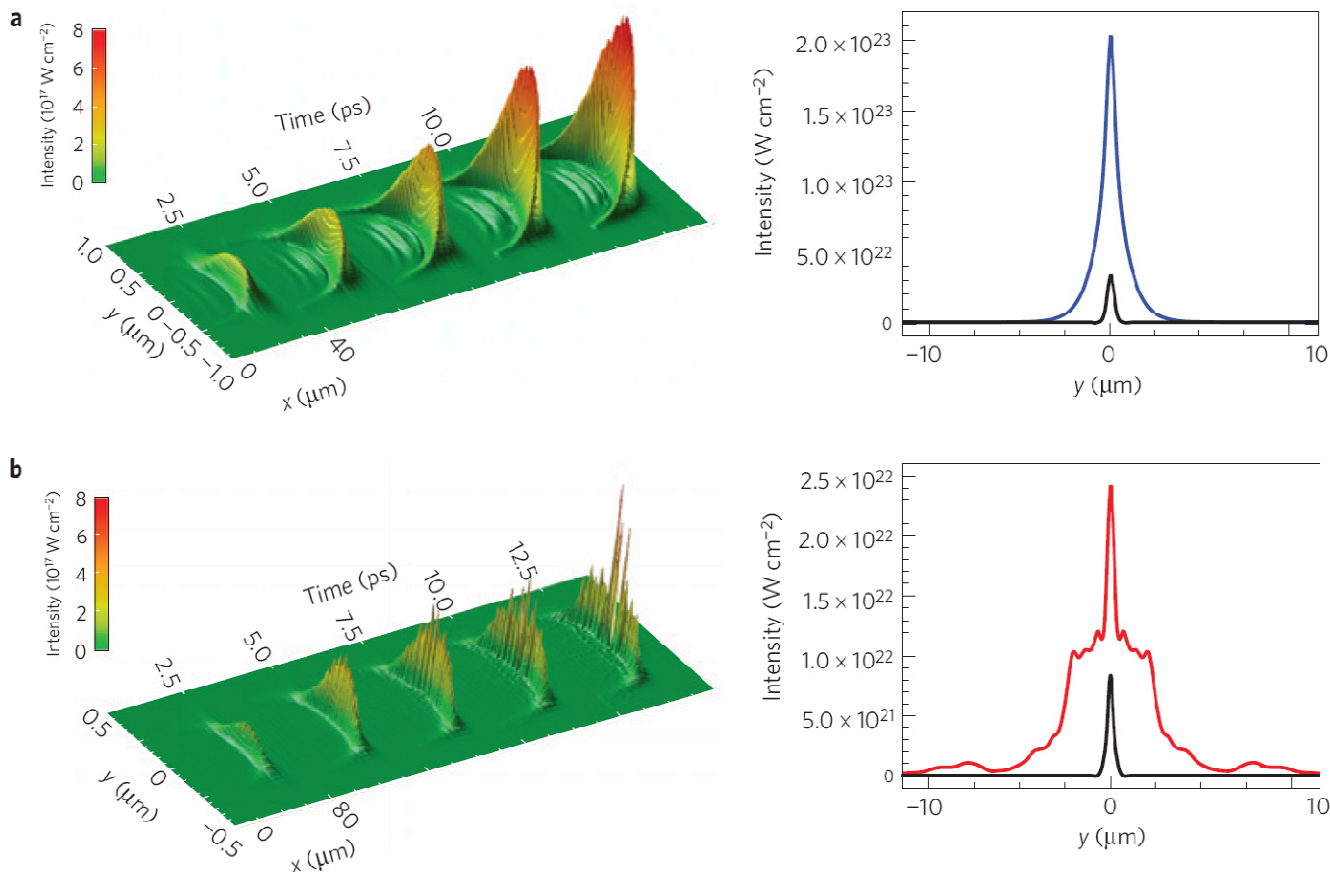


**Figure 6 Raman amplification of a short probe pulse under various conditions**

(a) Amplification under favourable conditions: pump intensity and plasma density are high enough to keep the process efficient, but not so high that instabilities can destroy the probe. The probe retains a smooth profile throughout the interaction (left), and its focused envelope is smooth with a narrow spot diameter (right). (b) Amplification under unfavourable conditions (plasma density is too high): the probe still grows, but it is broken up badly by instabilities (left). As a result, the focused envelope has a much larger spot diameter and is not smooth (right).

## 3.2 Timmy Ramirez-Cuesta, ISIS

### 3.2.1 *Studying the dynamics of hydrogen using Inelastic Neutron Scattering and Computer Modelling: Neutron Scattering and Hydrogen Storage*

Amongst the toughest challenges that we face at the beginning of the 21st century is the reduction of our dependence on fossil fuels and the global climate change implications. We know how to produce energy from a variety of sources, but we lack efficient ways of storing such energy. The most efficient way of storing energy is in its chemical form, in batteries or as hydrogen gas. The retrieval of the stored energy is straightforward in the case of the batteries but in the case of hydrogen requires an additional step that may be performed via fuel cell (conversion to electrical energy) or by burning (conversion to thermal energy). Hydrogen can store the most energy per unit weight of any element in the periodic table, and its potential applications as an energy vector are essentially unlimited. It can be used to store energy produced from sustainable energy sources during periods of low demand, that energy then used during periods of peak demand. However, as a gas, its volumetric energy density is very low. Consequently, it is a great imperative to identify methods of storing hydrogen in high gravimetric and volumetric densities.

The vibrational properties of solids and molecules are studied by spectroscopic methods. Infrared (IR) and Raman spectroscopies are well established optical techniques. Inelastic neutron scattering (INS) spectroscopy is another method of obtaining vibrational spectra that has the following advantages :

- INS spectroscopy is sensitive to the vibrations of hydrogen atoms; unlike Raman and infrared
- INS is not subject to optical selection rules. All vibrations are active and, in principle, measurable;
- INS observations are not restricted to the centre of the Brillouin zone (gamma point) as are the optical techniques;
- INS spectra are readily and accurately modelled using abinitio methods, making computer modelling indispensable to interpret experimental data.
- Neutrons penetrate deeply into materials and pass easily through the walls of metal containers, aluminium or stainless steel, making neutrons ideal to measure bulk properties of samples within controlled environments;
- INS spectrometers cover the whole range of the molecular vibration spectra, 0-500 meV (0-4000 cm<sup>-1</sup>).

The combination of computational modelling and INS spectroscopy is a very powerful tool to understand the behaviour of these systems. We have studied the dynamics of LiBH<sub>4</sub>, one of the highest hydrogen containing materials, using CASTEP, Raman, IR and TOSCA. We have characterised the transport mechanisms for hydrogen.

Another system that has generated great interest is NaAlH<sub>4</sub>, since this is the only hydrogen storage materials whose hydrogen adsorption and release properties have been catalysed, we used calculations and spectroscopy to identify the atomistic mechanisms of hydrogen mobility (see figure 7). A series of different solid state storage materials have been also investigated using this methodology.

Hydrogen can also be stored in its molecular form inside porous materials. In the last few years a new family of materials called MOFs (metal organic frameworks) has been invented. These materials have been studied with INS and DFT abinitio calculations at ISIS, . In particular, Al MIL53 is a porous structure that exhibits hysteresis as a function of temperature. The pores are closed at low temperatures and they open around room temperature creating 53% of the volume available for hydrogen molecules to get into the material. One of the ideas behind this mechanism is to tailor this behaviour to trap hydrogen at higher temperatures and lock it in place by cooling further down to liquid nitrogen temperatures (see figure 8).

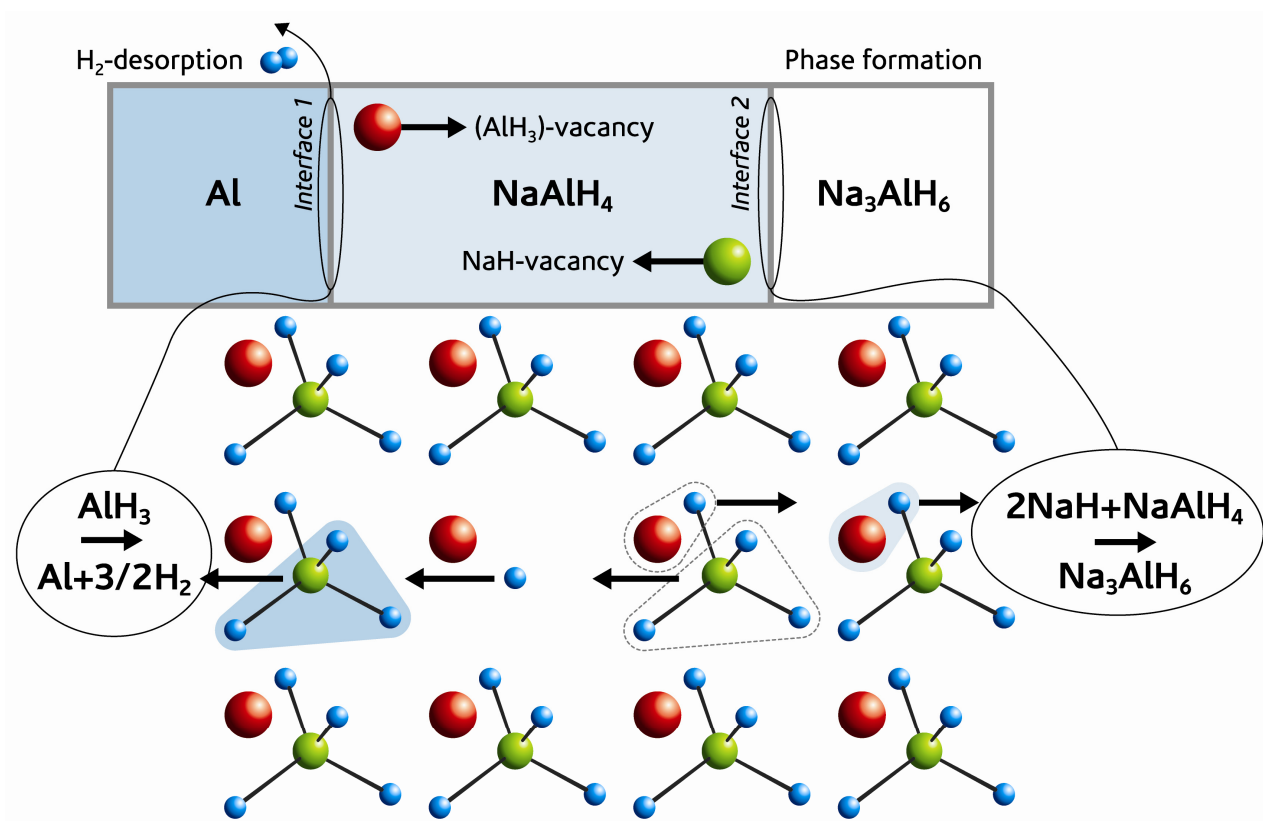
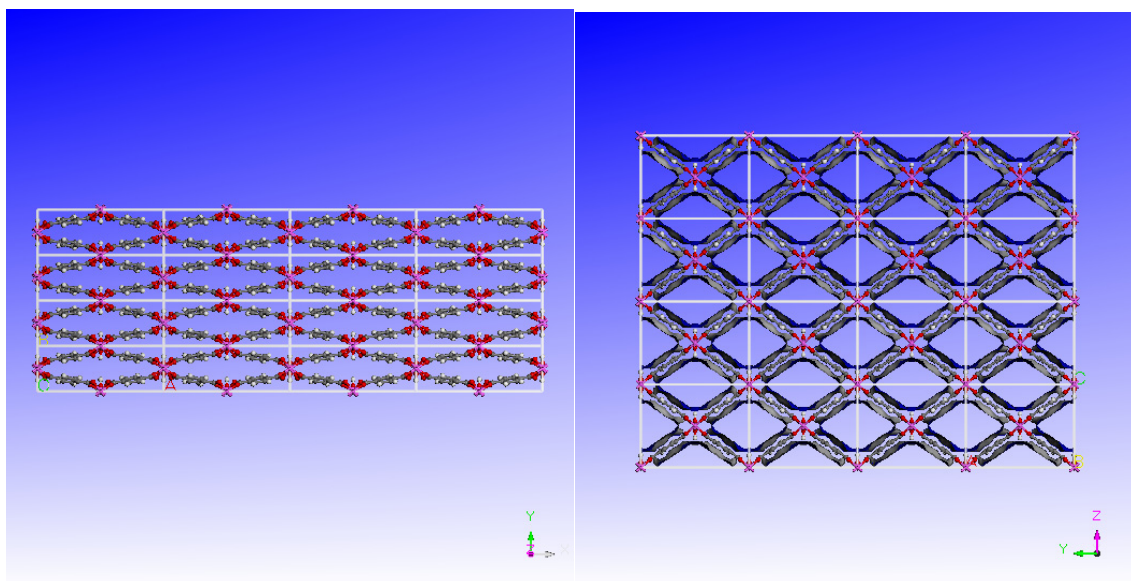


Figure 7 The proposed mechanism of hydrogen mobility inside TiCl doped NaAlH<sub>4</sub>



**Figure 8** The structure of Al MIL 53, left the closed structure that has no available volume for hydrogen adsorption, right the open pore structure with the Connolly surface representing the available volume for hydrogen adsorption

### 3.3 Stewart Parker, ISIS

#### 3.3.1 *Inelastic neutron scattering spectroscopy (INS)*

The ISIS Facility at RAL is the world-leading centre for vibrational spectroscopy of materials with neutrons: inelastic neutron scattering spectroscopy (INS). There are many ways to analyse INS data but the state-of-the-art is the comparison of spectra generated from ab initio calculations with experimental data. Increasingly, this is the standard that is required for publication.

For materials where the intermolecular forces are weak, the system can be treated as an isolated molecule and GAUSSIAN is generally used. The ability to use eight processors on SCARF for GAUSSIAN calculations and to have multiple calculations running simultaneously is a huge advantage. This was exploited to explore a wide range of spin states and geometries of possible compounds (36 in all) between iron atoms and dimers and benzene and enabled almost 40 years of disparate data to be resolved into a consistent description of the chemistry.

For systems where the intermolecular forces are significant, for extended systems or surfaces then CASTEP is the method of choice and in these cases SCARF is absolutely essential. A typical calculation will use 30-100 processors and take up to a week to complete. As an example, hydrous palladium oxide was investigated as a model system for a supported palladium catalyst. These are widely used for a variety of oxidation reactions including carbon monoxide removal from exhaust gas. For the calculations, a two layer slab was generated by cleavage of the literature structure of PdO along (001). This slab is oxygen terminated on one side and palladium terminated on the other. To avoid a polar solid, the oxygen terminated side was capped with hydrogen and the palladium side with hydroxyls. This creates a symmetrical slab that simplifies the calculations. The slab was then geometry optimised (the lattice parameters were fixed at those of bulk PdO) and a phonon calculation carried out, both to ensure that it was a stable system and to obtain the vibrational

spectra. A water molecule was then added to each side of the optimised slab, and the process repeated.

Figure 9 shows the result for the optimised system with the water molecule and a comparison of the experimental INS spectrum with those calculated for hydroxyl terminated slab and the water covered slab. Given the simplicity of the slab model, it can be seen that there is reasonable agreement between the observed and calculated spectra. In particular, it explains why only one strong band is seen in the INS spectrum of the partially dehydrated sample. The open nature of the surface means that displacement of the hydrogen atom either perpendicular or parallel to the surface results in a similar restoring force (since the only neighbouring atom is the oxygen that the hydroxyl is hydrogen bonded to) and hence similar transition energies. Introduction of the water molecule increases the amount of hydrogen bonding that the hydroxyl experiences and results in an upshift of the transition energies, as is commonly found.

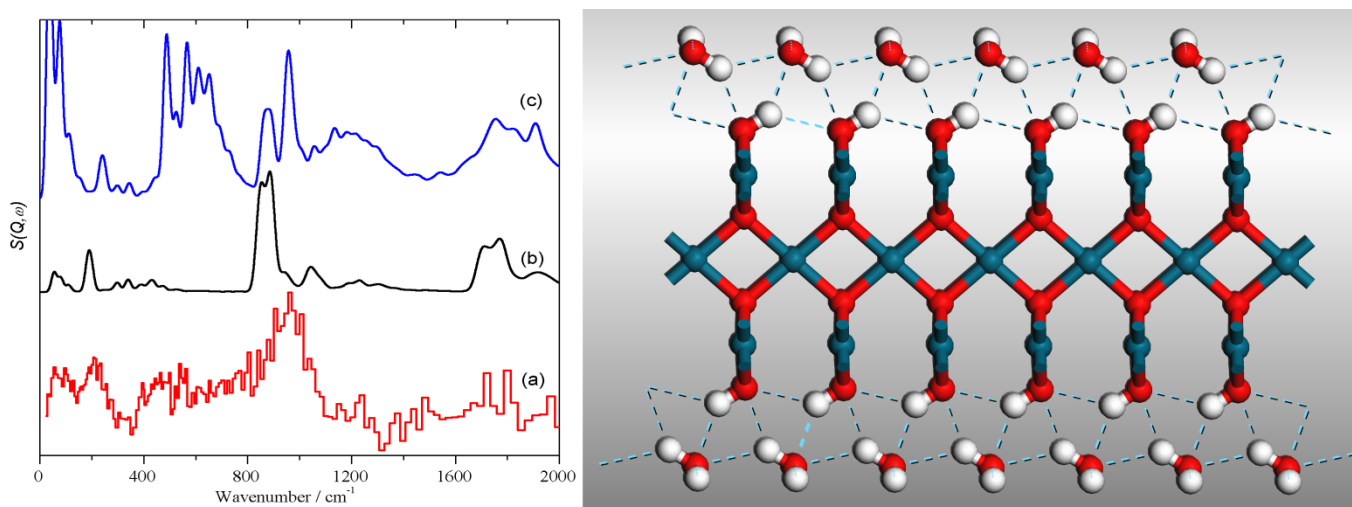


**Figure 9 Left: (a) experimental INS spectrum of partially dehydrated hydrous palladium oxide, (b) calculated INS spectrum for a hydroxyl terminated slab and (c) calculated INS spectrum for a water and hydroxyl terminated slab. Right: geometry optimised model obtained from the CASTEP calculations on SCARF used to generate (c).**

### 3.4 Sanghamitra Mukhopadhyay Imperial College London and STFC

#### 3.4.1 Investigation of new generation materials for solid oxide fuel cells (SOFCs).

Lanthanum cobalt oxide,  $\text{LaCoO}_3$ , is an industrially important material because of its use in high temperature solid oxide fuel cells (SOFCs) at around 1000K. Its thermodynamic stability and spin state transitions have been a subject of extensive study for decades. The material exhibits two transitions, around 100K and 500K. The first is from nonmagnetic semiconductor to paramagnetic semiconductor, and the second to paramagnetic metal. Although theoretical and experimental investigations have been reported, no consistent calculations have been done so far to address the thermodynamic stability and the electronic transition issues simultaneously. In the current work we used hybrid exchange density functional theory to calculate the electronic structure and vibrational frequencies, with which we compared the quasiharmonic free energies of five possible phases as a function of temperature. We have used first principle thermodynamics with hybrid exchange functional and Gaussian type localised basis sets. We have used CRYSTAL09 program for our calculations. Our calculations show that thermodynamic stability of a spin ordered mixed spin state at the intermediate temperature range can explain the magnetic insulator state of the material. The

calculated structural parameters, vibrational frequencies and magnetic moments have been compared with experiments.

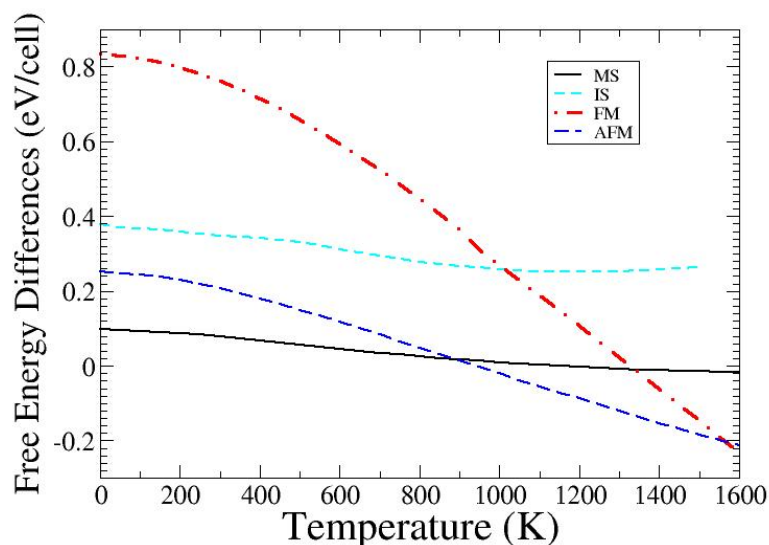


**Figure 10.** Difference of quasi-harmonic free energies for five different spin states of LaCoO<sub>3</sub> with respect to the low spin state, where five candidate magnetic states of Co were considered within a unit cell containing two Co atoms, namely low spin (LS,  $t_{2g}^6 e_g^0$ ,  $S = 0$ ), mixed spin (MS, a 50% mixture of  $t_{2g}^4 e_g^2$ ,  $S = 2$ , and  $t_{2g}^6 e_g^0$ ,  $S = 0$   $\text{Co}^{+3}$  ions), intermediate spin (IS,  $t_{2g}^5 e_g^1$ ,  $S = 1$ ), high spin (HS,  $t_{2g}^4 e_g^2$ ,  $S = 2$ ) ferromagnetic (FM) and HS antiferromagnetic (AFM). A rhombohedral unit cell of R-3C symmetry was assumed.

### 3.4.2 Investigation on Mn doped Silicon for spintronics Applications

Electronics is on the brink of a revolution that will see complementary metal oxide semiconductor (CMOS) electronics replaced by spintronics in which device performance depends on the electronic spin. It is possible that Moore's law can be maintained for another two decades with gate lengths dropping to roughly 5nm before fundamental physical limits are reached. Quantum devices, which exploit the spin of electrons can be smaller than 1nm. This is why the post-CMOS era will be based on spintronics in semiconducting materials that are ferromagnetic at room temperature. The need to retain the current technology base is a major driving force for the development of innovative approaches to render Silicon ferromagnetic at room temperature. Mn implanted Si is of potential technological importance as a ferromagnetic semiconductor capable of supporting strongly spin-polarised electron transport. The detailed mechanism of magnetic interaction and the role of background carriers in Mn doped Si is unclear. We have used hybrid exchange density functional methods to investigate the electronic properties of Mn doped Si. The role of background carrier has been implemented by introducing extra positive or negative charge in the unit cell. A constant charge of opposite polarity has been used to maintain the neutrality of the unit cell. Our calculation shows that the p-type background charge helps to stabilize a ferromagnetic state but n-type background charge not. In the former case a strong p-d coupling between Si and Mn has been identified as the reason. The calculated results agree well with experiments.

### 3.4.3 First principle simulations of AlF3 surfaces

Aluminium fluoride (AlF3) is an industrially important material because of its use as catalyst in the dismutation reactions of chlorofluorocarbon. We have investigated the surface of the material using first principle density functional method using hybrid exchange functional. We have used B3LYP functional and Gaussian type localised basis set. We already have published a series of papers on this subject in last few years. Currently we are investigating the electronic structures and the transition path of the catalytic reactions on the AlF3 surfaces.

## 3.5 Mark Quinn, Strathclyde University

### 3.5.1 Ultra-intense laser-solid interactions and fast electron transport in solid density plasma

In the interaction of an intense laser pulse with a solid target a significant fraction of the laser energy is converted into a population of relativistic (fast) electrons. The physics of the transport of these electrons in the ensuing dense plasma is important in a number of related topics in the field of high power laser-plasma physics. Key amongst these is the potential to use fast electrons to transfer energy for the Fast Ignition approach to Inertial Confinement Fusion and to accelerate ion beams to multi-MeV energies.

A number of investigations of electron transport and ion acceleration have been carried out using the SCARF e-Science facility at RAL. These investigations have used sophisticated numerical modelling to study:

- (i) the effects of self generated magnetic fields on electron beam divergence,
- (ii) the role of ion ordering and electron-ion scattering in electron beam filamentation,
- (iii) the influence of electron refluxing on electron transport measurements,
- (iv) and the discovery of a novel laser absorption mechanism

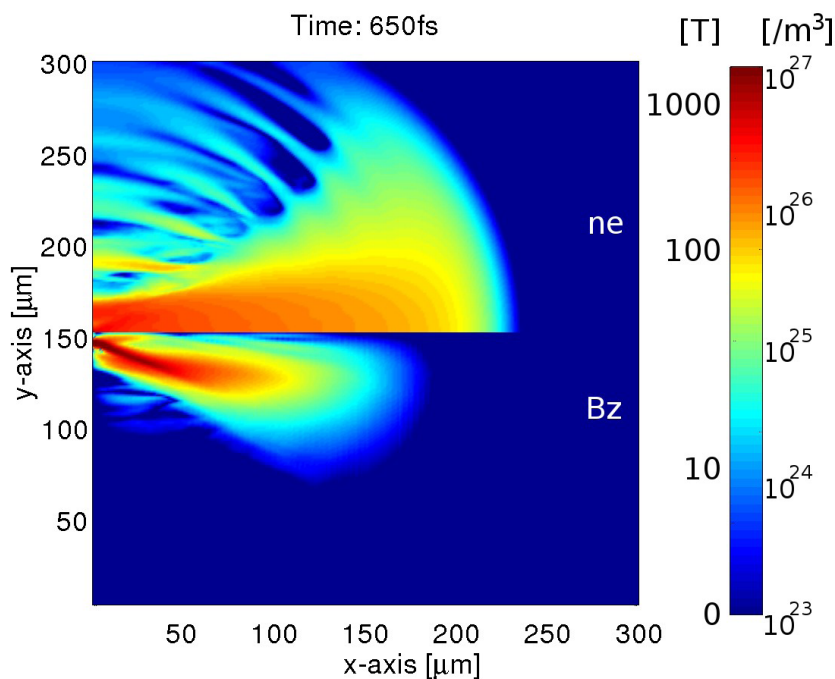


**Figure 11** Simulation of fast electron transport in a 300 μm Aluminium target using LEDA. The fast electron density (ne) and the self-generated azimuthal magnetic field (Bz) are shown at time 650 fs since laser incidence. The electron beam is injected from the left hand side and propagates along the x-direction.

### 3.6 Stephen Brooks, AsTeC

#### 3.6.1 *Optimising Pion Production Target Shapes for the Neutrino Factory*

The neutrino factory requires a source of pions within a momentum window determined by the ‘muon front end’ accelerator structure downstream. The technique of finding which parts of a large target block are net absorbers or emitters of particles may be adapted with this momentum window in mind. Therefore, analysis of a hadronic production simulation run using MARS15 can provide a candidate target shape in a single pass. However, changing the shape of the material also affects the absorption/emission balance, so this paper investigates iterative schemes to find a self-consistent optimal, or near-optimal, target geometry.

#### 3.6.2 *First Sequence –only removing material*

Starting with a solid cylinder of tantalum 1m long and 10cm in radius, successive MARS simulations identify the parts that are net producers and absorbers of useful pions. On each iteration, the parts that are net absorbers are removed.

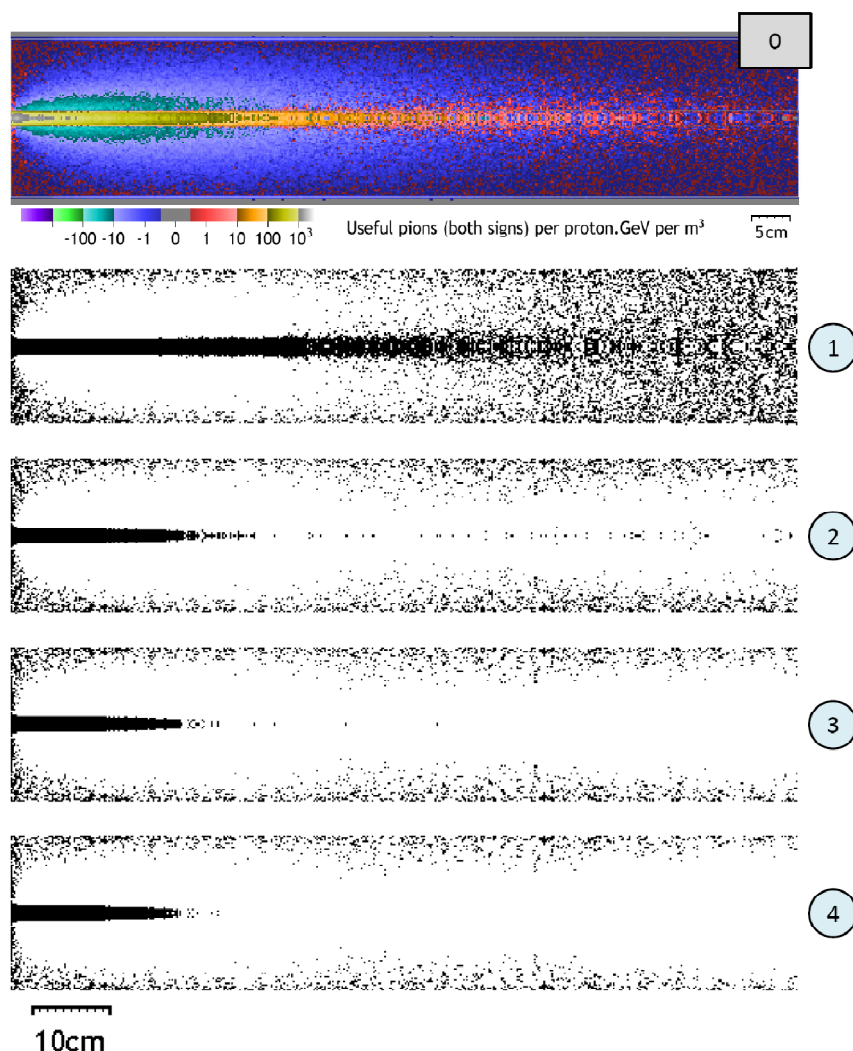


Figure 12: The first picture shows the pion balance in the original solid cylindrical block, the rest, from top to bottom show geometries 1 through 4

### 3.7 Matthew Krzystyniak, ISIS

#### 3.7.1 *Software Tools for comparing ab initio calculated proton dynamical features with the results of neutron spectroscopic studies*

The main use of SCARF cluster has been in connection with the realization of an extensive research project in neutron spectroscopy. The project aims at developing software tools and methods to compare and contrast ab initio calculated proton dynamical features with the results of neutron spectroscopic studies using neutron Compton scattering (NCS), quasi elastic scattering (QENS) and inelastic scattering (INS) in condensed matter and molecules.

Two major programs have been used Gaussian 03 and CASTEP, both quantum chemistry software packages. The Gaussian was used within the license purchased by the STFC and the PW-DFT code CASTEP was used as a piece of software co-developed at the Rutherford Labs by CASTEP Development group, a part of UK Car Parrinello Consortium.

The methodology was develop own software tools (in Fortran and Matlab) that would serve as an interface between the quantum chemistry results and the neutron spectral simulations. The software has been largely developed and tested so far. It performs input parsing from the output of ab initio programs, the calculation of relevant observables and simulation and fitting of neutron NCS and INS spectra to the spectra recorded. Vibrational density of states (VDOS), total and partial/projected are calculated based on linear response theory or the finite-displacement method. The VDOS can then be convoluted with instrument resolution function and directly compared with INS spectra. In case of NCS the VDOS serves as basis for the calculation of the nuclear momentum distribution and the mean proton kinetic energies. These first-principles predictions of Compton profiles have been done for the first time in the whole literature on the subject, with important ramifications for substances like proton storage materials and protons conductors, systems with hydrogen bonds and biological systems.

The successful application of this methodology redefines the position of STFC at the forefront of neutron research as far as material properties are concerned. Important examples realized so far are model calculations in ammonium hexachlorometallates, [Krzystyniak M, Lalowicz ZT, Chatzidimitriou-Dreismann CA, Lerch M, J. Phys. Condens. Matter, 21, 075502, (2009)], hydrogen bonding systems, liquid and solid hydrogen fluoride (HF) [Matthew Krzystyniak, J. Chem. Phys, in press (2010)] and calculations in hydrogen storage and proton conducting system, lithium hydride and lithium deuteride (LiH and LiD) [Matthew. Krzystyniak et al, Phys. Rev. B, in preparation].

Neutron Compton scattering (NCS) measurements on ammonium hexachloropalladate and hexachlorotellurate were performed at room temperature. Proton scattering intensities and momentum distributions, as measured in the NCS experiment, have been compared with results expected from the impulse approximation (IA) for both systems. The measurement shows that scattering intensity from protons is anomalous even though their momentum distribution has a second moment that agrees very well with the ab initio calculation for an isolated pseudo-spherical NH<sub>4</sub><sup>+</sup> ion in the ground vibrational state. Detailed data analysis shows that there is no extra (beyond the IA expected value) broadening or peak shift of proton momentum distribution due to ultra-fast kinetics of the Compton scattering process leading to anomalous scattering intensities. This is most probably due to highly symmetric local potential in the NH<sub>4</sub><sup>+</sup>. Presented results have interesting implications for further theoretical work in the field.

Neutron Compton scattering (NCS) experiments were performed on liquid and solid HF, a system where the effective Born-Oppenheimer (BO) potential energy surface is not isotropic. Proton momentum distributions were calculated in the framework of the impulse approximation from measured neutron Compton profiles. A detailed data analysis shows that there are no systematic changes in the width, position of the maximum, or excess kurtosis of proton momentum distributions in both systems with increasing scattering angle. This observation has important implications for further theoretical work on violation of BO approximation in the presence of ultrafast neutron-proton scattering. That is, the picture of proton dynamics in HF emerging from the analysis of NCS data does not seem to support

the previously considered model of protons accessing excited electronic states due to ultrafast scattering. A calculation of nuclear momentum distribution of liquid and solid hydrogen fluoride was performed. In both systems, density functional theory generalized gradient approximation functional of Perdew, Burke and Ernzerhof was used for the calculation: for liquid hydrogen fluoride, using an atom centered basis set for an isolated molecule with optimized geometry, and for solid hydrogen fluoride using plane wave basis sets on optimized orthorhombic crystal cell. For liquid hydrogen fluoride, a semi classical approach was adopted with the vibrational contribution to momentum distribution obtained from the density functional theory calculation and translational and rotational contributions calculated classically. Nuclear momentum distribution in the solid hydrogen fluoride was calculated entirely quantum mechanically using phonon dispersion and vibrational density of states calculated in the framework of plane wave density functional theory. Theoretical results were contrasted with recently obtained results of Compton (deep inelastic) neutron scattering on liquid and solid hydrogen fluoride. In case of liquid hydrogen fluoride, almost a perfect agreement between theory and experiment was achieved within the harmonic Born-Oppenheimer approximation. For the solid system under investigation, the harmonic approximation leads to small (4%) overestimation of the square root of the second moment indicating that neutron Compton scattering technique is sensitive to proton delocalization due to hydrogen bonding in solid hydrogen fluoride.

In case of Lithium Hydride and Lithium Deuteride similar conclusions as for HF have been reached. Namely, the ab initio calculated VDOS and momentum distributions from plane wave DFT for ground state electronic wave functions agree surprisingly well with experimental results from NCS supporting the idea of the lack of electronic excitation in the ultra fast scattering process.

In the future, ab-initio Born-Oppenheimer Molecular Dynamics (BO – MD) and Path Integral Molecular Dynamics (PI - MD) methods will be used to calculate the ensemble average proton position and its correlation functions. These will be used to extract diffusion coefficients and proton mobility to be compared with the QENS, INS and NCS measurements.

### **3.8 Keith Refson, CSE**

#### **3.8.1 *Plane-wave Materials Simulation on SCARF with CASTEP***

Materials modelling based on periodic density-functional theory (DFT) using a plane-wave basis set and pseudopotentials is one of the most influential methods in computational science. Since the seminal paper of Car and Parrinello implementations have used grid-based, fast Fourier transform (FFT) methods to achieve very high performance, allowing routine modelling of systems containing

hundreds of atoms. CASTEP is the UK's premier plane-wave DFT modelling code, and pioneered the implementation and use with HPC resources, and is one of the most heavily used codes on national HPC resources as well as on SCARF.

The power and high-availability of an HPC facility such as SCARF is essential to the CSED science programme, and STFC's scientific profile. A strong component of DFT simulation using CASTEP has marked the programmes on light alloy materials for automotive hydrogen storage applications, catalysis, functional materials, and fundamental systems such as the quantum critical magnet MnSi. A particularly strong example is the collaboration with the ISIS spectroscopy group which has resulted in 5 scientific publications in 2009/2010 on spectroscopic studies of catalysts, hydrogen storage materials, and molecular organic crystals.

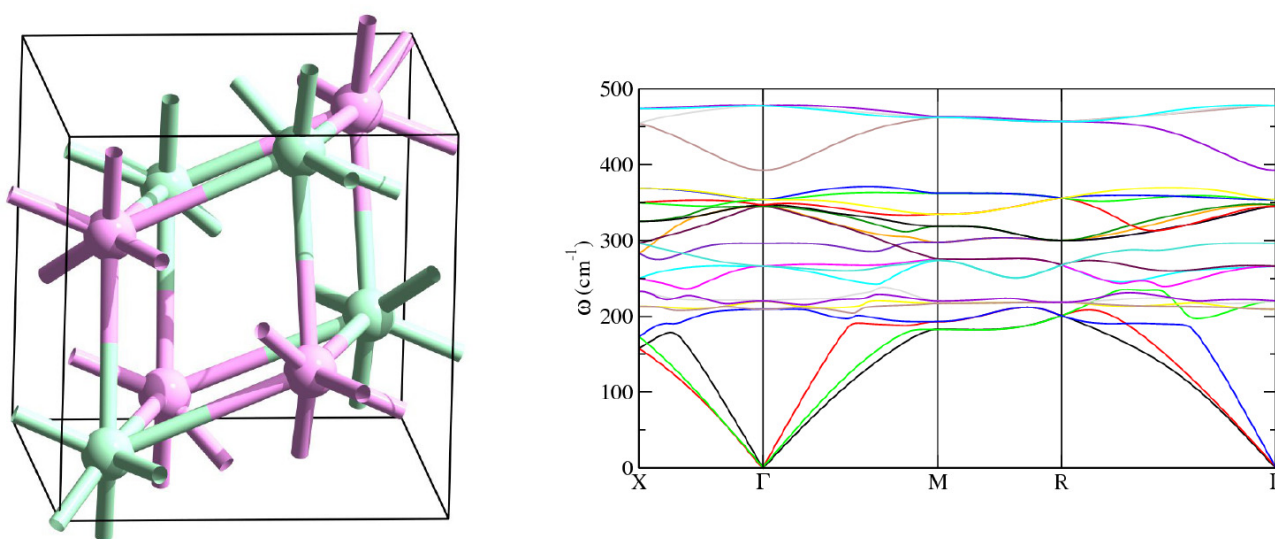


**Figure 13: The structure of the quantum critical magnet, MnSi and phonon dispersion curves calculated on SCARF.**

SCARF has also proved invaluable in promoting STFC's training mission; the ISIS neutron training course (in May 2010) contained a computational day in which 8 postgraduate students learned the power of DFT simulation with CASTEP in a hands-on session using SCARF.

### 3.9 Iain McKenzie, ISIS

#### 3.9.1 *Muoniated Spin Probes in Soft Matter*

My research involves calculating the structure, energetics and hyperfine coupling constants of muoniated radicals using the Gaussian 03 package of programs. These calculations are used to aid the assignment of muon spin rotation / relaxation / resonance spectra obtained using the ISIS muon spectrometers (HiFi, EMU and MuSR) and assist in evaluating new systems for investigation. I have recently demonstrated that the report Drew et al. Phys. Rev. Lett. 2008, 100, 116601) to have measured the intrinsic conductivity of organic semiconductors using muon spin relaxation is incorrect and that the muon pins the unpaired electron rather than allowing it to diffuse. My results are important as several research groups have proposed to use muon spin relaxation to measure charge transport properties in similar materials and this will allow better use of facility time.

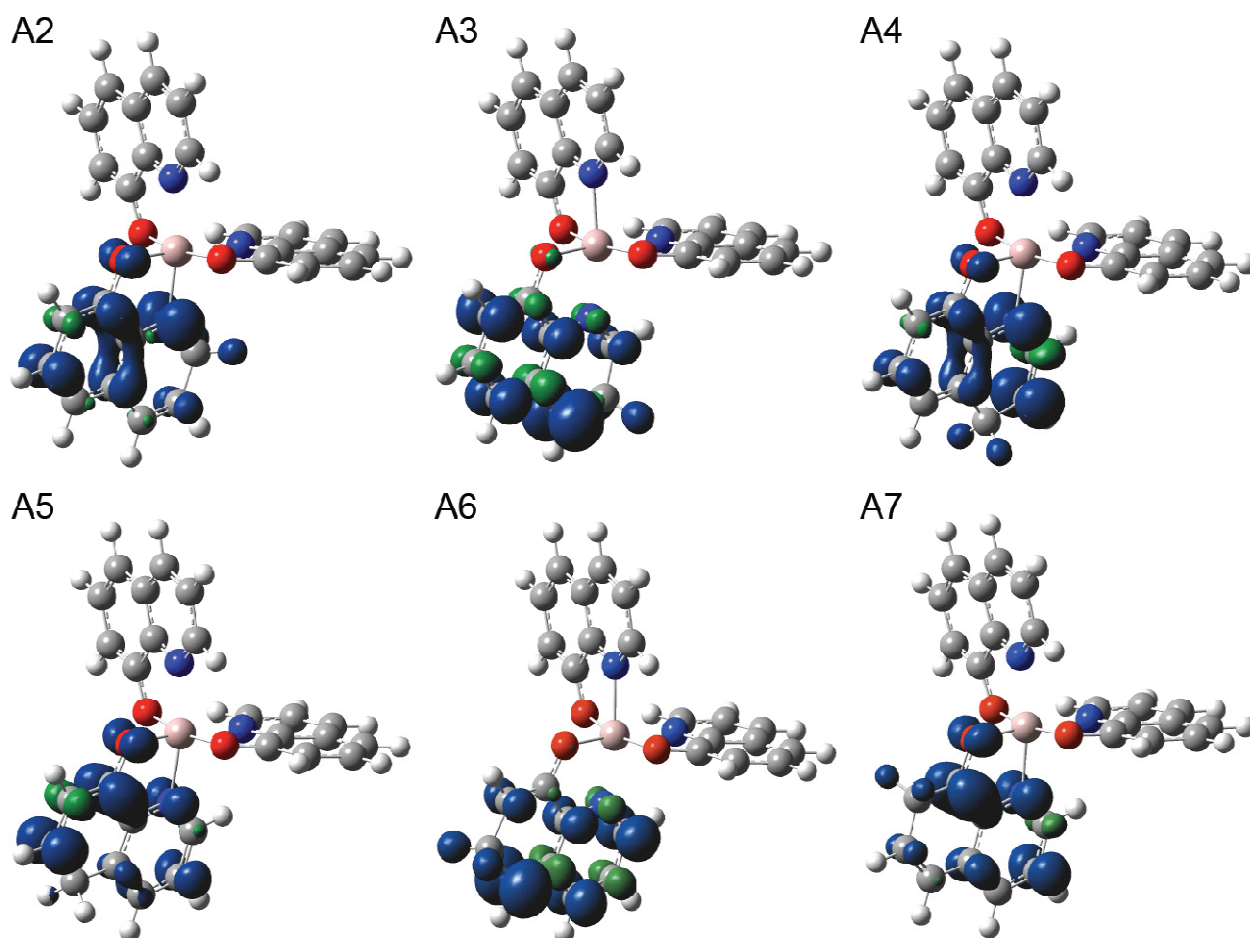


Figure 14: The image shows the unpaired electron spin density distribution in some of the muonium adducts of Alq3, a molecular semiconductor

### 3.10 Rowan Hargreaves (ISIS), Karen Edler (Bath) and Daniel Bowron (ISIS)

#### 3.10.1 Using Empirical Potential Structure Refinement (EPSR) to model *n*-Decyltrimethylammonium (C10TAB) Bromide micelles

Periodic mesoporous silica (PMS) materials are an important class of material as they can be used as molecular sieves and catalysts, and are being used in drug delivery, membrane separation and a number host-guest chemistry processes. PMS materials are formed using a micelle-template method: micelles are formed by the self-assembly of surfactant molecules in aqueous solution, then a source of silica is added, the silica then forms a scaffold around the micelles, and once the silica has condensed the surfactant molecules can be removed, leaving a material containing ordered nano- or meso-pores. The pores formed can be tuned because the size and morphology of the aggregates formed by the surfactants vary with type and concentration of the surfactant, the temperature, the pH, and the nature of the solvent and counter-ion present.

Developing a precise understanding of this templating process, specifically the role of the solvent and counter-ion on the micelles, is required to aid the design of PMS materials.

I have used SCARF to run Empirical Potential Structure Refinement (EPSR) simulations to produce atomistic models of neutron diffraction data on a series of isotopic substituted 0.4M aqueous solutions of C10TAB surfactant molecules with bromide counter ions taken on the SANDALS diffractometer at ISIS.

EPSR uses Monte Carlo (MC) simulation approach to evolve configurations of atoms through phase space, but in addition to the usual interaction potentials used in classical atomistic molecular modelling an empirical potential (EP) is included. The EP reflects the difference between the measured diffraction data and that calculated from the current configuration of atoms in the simulation would produce. In this way an EPSR model should produce configurations that are consistent with experimental measurement of the real system's structure.

The largest simulations I ran contained 64 surfactant molecules and counter ions and 7808 water molecules, giving a total of 26,304 atoms in a cubic box with sides of length 64.5 Å. This size is about the maximum size of simulation that is currently feasible with EPSR, but is sufficient to contain one complete micelle and some oligomers of surfactant molecules (at this concentration it is thought that the micelles contain about 30 to 40 molecules).

The simulations were started from initially disordered configurations, as the simulations proceeded aggregates formed containing up to 55 surfactant molecules -- Figure 15 shows an example of a micelle formed. For comparison I ran some MC simulations that were not refined against the experimental data, and these did not contain anywhere near the same proportion of large aggregates as those refined against the data. This indicates that introducing the empirical potential allows the system to explore phase space much faster (at least 3 times faster). Despite this speed up, it was necessary to run a series of simulations each started from a different initial configuration to improve the sampling of these large structures and their local environment.

Figure 16 shows the distribution of the different atomic species from the centre of mass of micelles containing 20 or more surfactant molecules. It shows that the internal part of the micelle contains the tail groups of the surfactant molecules and the headgroups are to the outside. Interestingly it seems that both the bromide ions and water molecules encroach into the headgroup part of the micelle and that bromide ions are not strongly bound to the micelle but are distributed throughout the solution.

These simulations are just a preliminary part of this study since other diffraction experiments have been performed investigating the effect of temperature, pH and surfactant concentration, and the effect of adding a source of silica. There is considerable scope for performing further large scale EPSR simulations for this project, and for some of the other science being done on NIMROD and SANDALS diffractometers.

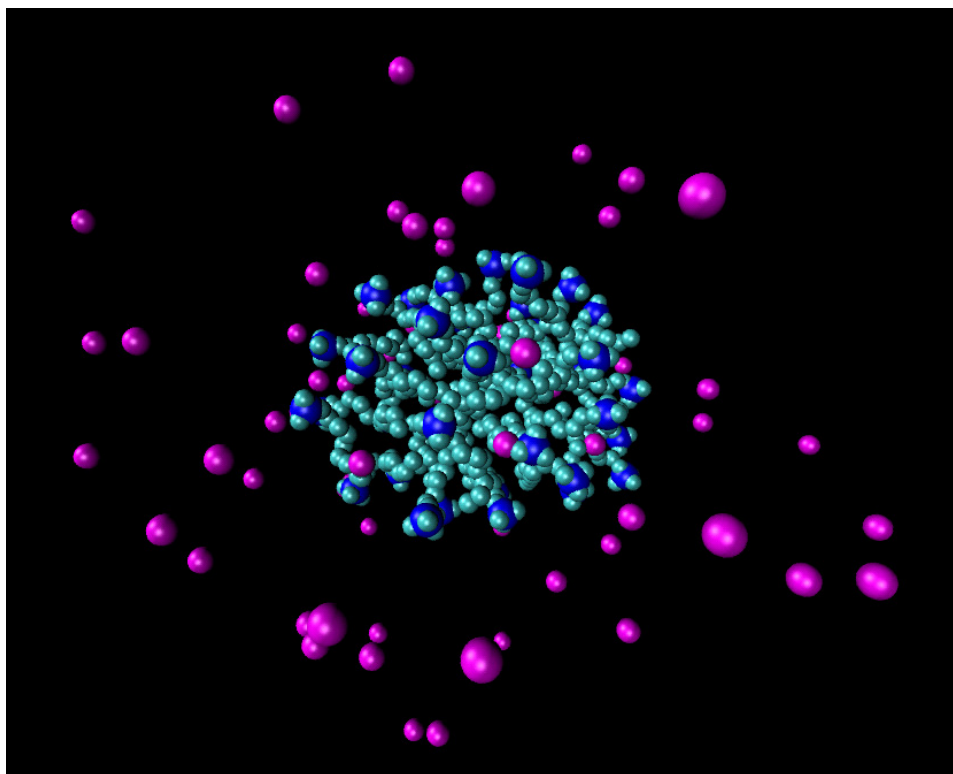


Figure 15: A micelle composed of 41 C10TAB surfactant molecules. The carbon atoms shown in cyan, with the nitrogen atom in the headgroups shown in blue, and the bromide ions are shown in magenta. The water molecules and the other surfactant molecules present in the simulation are not shown.

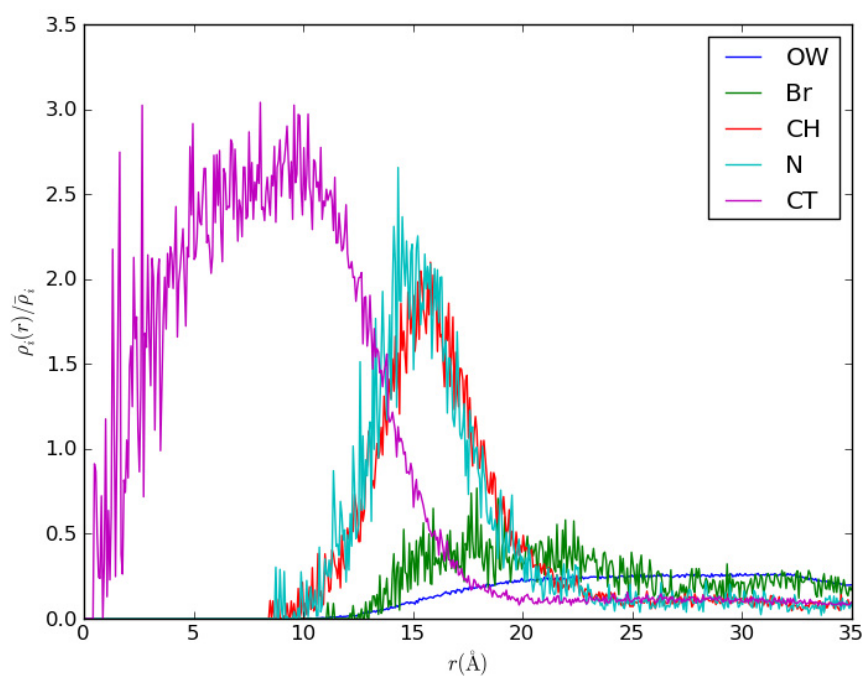


Figure 16: The radial distribution of the relative number density of different atom types from the centre of mass of micelles containing more than 20 surfactant molecules. The atom types are: OW – oxygen in the water molecules; Br – the bromide ions; CH – the carbon atoms in the surfactant headgroup; N – the nitrogen atom in the surfactant headgroup; and CT the carbon atoms in the tail groups of the surfactant molecules.

### **3.11 David Royse ISIS**

#### ***3.11.1 Geometry optimisations and phonon calculations***

My use of SCARF has been under the supervision of Professor Bill David and Dr Timmy Ramirez-Cuesta. Presently most of the work has been using CASTEP and involved simple geometry optimisations and phonon calculations. These have been used to simulate INS data collected on TOSCA. At this time, no publications have arisen from this work but we are working on three drafts that we hope will be published soon.

This work has focussed on two groups of materials, the first  $\text{Li}(\text{NH}_3)_n\text{BH}_4$  is a promising ammonia storage material and shows some potential as a useful hydrogen storage material. We are currently modelling this compound with the hope of fully understanding the circumstances under which it releases ammonia or hydrogen. The compound  $\text{Li}(\text{NH}_3)_n\text{BH}_4$  forms phases with  $n = 0, 1, 2, 3$  and  $4$  which we have investigated using GEM and HRPD, very preliminary work in calculating the optimised versions of these structures has begun, and we hope that combined with molecular dynamic calculations will form the basis of a second paper.

A second group of compounds,  $\text{Mg}(\text{NH}_3)_6\text{X}_2$  where X is a halide, have also received much attention as potential ammonia stores. Using SCARF we have begun the process of modelling these systems in order to fully understand their INS spectra that we have collected on TOSCA. Modelling these systems is not as simple as it may first appear. This is because of the significant disorder present within the structures, our calculations and low temperature experiments show that this disorder is present to very low temperatures.

### **3.12 Dean Adams ISIS Accelerator Physics Group**

#### ***3.12.1 Particle Tracking using ORBIT***

The ISIS synchrotron is a high intensity proton accelerator at the Rutherford Appleton Laboratory and forms part of the accelerator complex. Safe reliable operation of the synchrotron requires high levels of proton beam control. Proton beam loss leads to machine component activation which inhibits hands on maintenance.

The SCARF-IBIS cluster is used to run the particle tracking code ORBIT. This code allows the ISIS Accelerator Physics group to run simulations of many aspects of machine operation. These include injection, beam trapping, acceleration, the influence of 1d, 2d and 3d space charge. Real machine apertures and collimation systems can also be included to produce beam loss dynamics which can be compared to real measurements. Resonance analysis due most common lattice errors, such as the half integer, allow the group to study the effects of emittance blowup, halo formation and tune depression. Typical beam simulations require 600K particles and can take 24 hours on 64 cpu's to track approximately 3,000 turns of the 12,000 turn ISIS acceleration cycle. Figure 17 below shows the beam distributions at turn 1000 of the acceleration cycle. The bottom left plot shows an un-trapped beam which will ultimately lead to beam loss.

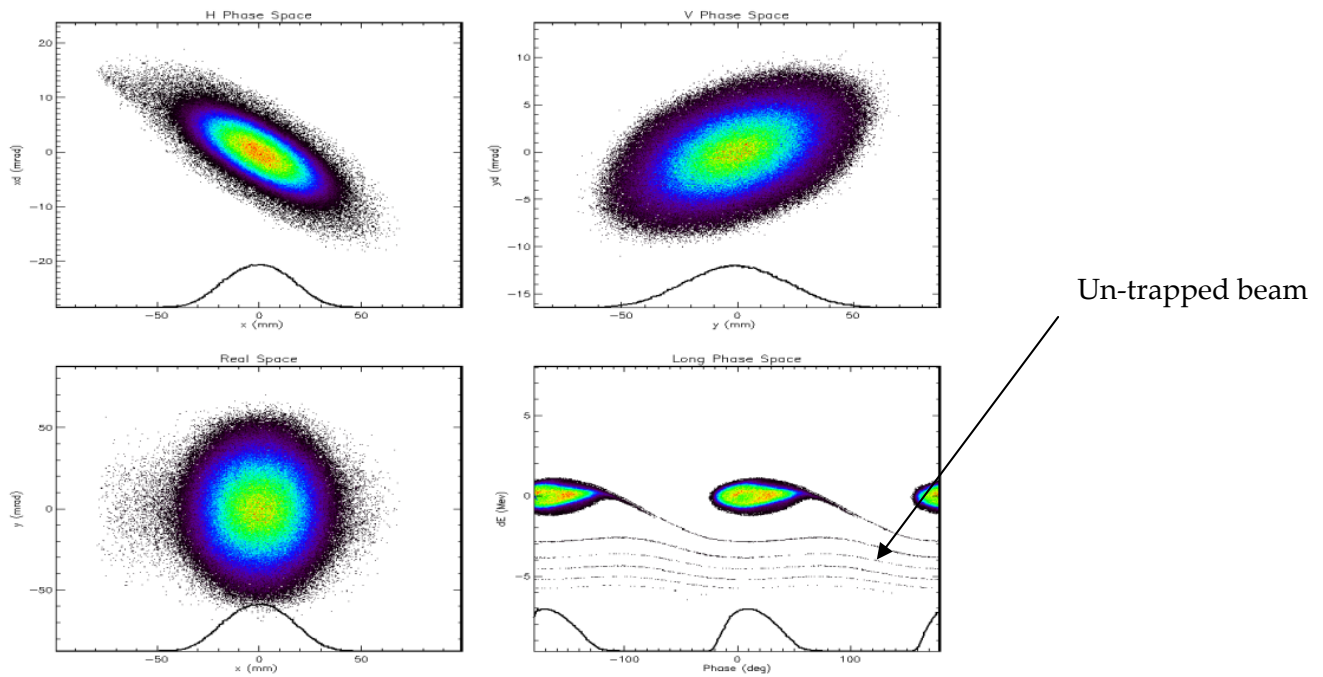


**Figure 17: Typical plot of proton beam distributions calculated in ORBIT. In clockwise order from top left they are, horizontal phase space, vertical phase space, real space and longitudinal phase space.**

ISIS has recently installed 4 new accelerating cavities to provide and beam intensity increase. ORBIT simulations are providing valuable insight in understanding new temporal beam loss distribution and into diagnosing hardware setup issues.

The MICE (Muon Ionisation Cooling Experiment) facility in operation on the ISIS synchrotron creates muons by dipping a target into the circulation proton beam. ORBIT simulations are being used to calculate spatial beam loss distributions for comparison with measurement.

A potential upgrade to ISIS is to increase the synchrotron injection energy from 70 MeV to 180 MeV by replacing the linac. ORBIT is being used to calculate the new injection system requirements and predict the ultimate achievable intensity.

1. APPENDIX : SCARF HARDWARE DETAILS

Host group	CPU type and frequency	Nodes	Cores /node	Total cores	Interconnect	Total memory
Lexicon-2/ SCARF10	Intel E5530 @ 2.40GHz	104	8	832	DDR Infiniband	2496 GB
IBIS/ SCARF09	Intel E5462 @ 2.80GHz	48	8	384	SDR Infiniband	768 GB
SCARF08	Intel E5430 @ 2.66GHz	46	8	368	SDR Infiniband	736 GB
Lexican/ SCARF07	AMD Opteron 275 @ 2.2GHz	73	4	292	GB Ethernet	584 GB
General/ SCARF06	AMD Opteron 285 @ 2.6GHz	50	4	200	Myrinet	400 GB
<b>Grand Totals</b>		321		2076		4984GB

2. APPENDIX: INDEX OF FIGURES

Figure 1 Pie chart showing percentage usage of the SCARF service by department ..... 3

Figure 2: Availability for SCARF ..... 4

Figure 3: Availability vs Year Purchased ..... 4

Figure 4 Slice through the Magnetic Switchyard ..... 6

Figure 5 Fast Electron Flow through Magnetic Switchyard . Fast Electrons enter as hemispherically divergent flow and are focussed into a beam ..... 6

Figure 6 Raman amplification of a short probe pulse under various conditions ..... 7

Figure 7 The proposed mechanism of hydrogen mobility inside TiCl doped NaAlH4 ..... 9

Figure 8 The structure of Al MIL 53, left the closed structure that has no available volume for hydrogen adsorption, right the open pore structure with the Connolly surface representing the available volume for hydrogen adsorption ..... 10

Figure 9 Left: (a) experimental INS spectrum of partially dehydrated hydrous palladium oxide, (b) calculated INS spectrum for a hydroxyl terminated slab and (c) calculated INS spectrum for a water and hydroxyl terminated slab. Right: geometry optimised model obtained from the CASTEP calculations on SCARF used to generate (c) ..... 11

Figure 10. Difference of quasiharmonic free energies for five different spin states of LaCoO3 with respect to the low spin state, where five candidate magnetic states of Co were considered within a unit cell containing two Co atoms, namely low spin ( LS,  $t_{2g}^6e_g^0$ , S = 0), mixed spin (MS, a 50% mixture of  $t_{2g}^4e_g^2$ , S=2, and  $t_{2g}^6e_g^0$ , S = 0 Co<sup>+3</sup> ions), intermediate spin ( IS,  $t_{2g}^5e_g^1$ , S=1) , high spin (HS,  $t_{2g}^4e_g^2$ , S=2) ferromagnetic (FM) and HS antiferromagnetic (AFM). A rhombohedral unit cell of R-3C symmetry was assumed. .... 12

Figure 11 Simulation of fast electron transport in a 300 μm Aluminium target using LEDA. The fast electron density (ne) and the self-generated azimuthal magnetic field (Bz) are shown at time 650 fs since laser incidence. The electron beam is injected from the left hand side and propagates along the x-direction. .... 13

Figure 12: The first picture shows the pion balance in the original solid cylindrical block, the rest, from top to bottom show geometries 1 through 4 ..... 14

Figure 13: The structure of the quantum critical magnet, MnSi and phonon dispersion curves calculated on SCARF ..... 17

Figure 14: The image shows the unpaired electron spin density distribution in some of the muonium adducts of Alq3, a molecular semiconductor ..... 18

Figure 16: The radial distribution of the relative number density of different atom types from the centre of mass of micelles containing more than 20 surfactant molecules. The atom types are: OW – oxygen in the water molecules; Br – the bromide ions; CH – the carbon atoms in the surfactant headgroup; N – the nitrogen atom in the surfactant headgroup; and CT the carbon atoms in the tail groups of the surfactant molecules. .... 20

Figure 15: A micelle composed of 41 C10TAB surfactant molecules. The carbon atoms shown in cyan, with the nitrogen atom in the headgroups shown in blue, and the bromide ions are shown in magenta. The water molecules and the other surfactant molecules present in the simulation are not shown. .... 20

Figure 17: Typical plot of proton beam distributions calculated in ORBIT. In clockwise order from top left they are, horizontal phase space, vertical phase space, real space and longitudinal phase space. .... 22

## 3. APPENDIX: PUBLICATIONS AND PRESENTATIONS

#	Reference	Department
1.	High Intensity studies of the ISIS Synchrotron .... C Warsop et al, HB2010	Dean Adams, ISIS
2.	Injection Upgrade on the ISIS Synchrotron – B. Jones et al, IPAC2010	Dean Adams, ISIS
3.	The MICE muon beam: Status and Progress – D Adams IPAC10	Dean Adams, ISIS
4.	Space Charge and High Intensity Studies ISIS – C.Warsop et al, B2008	Dean Adams, ISIS
5.	Injection Optimisation on the ISIS Synchrotron – B. Jones et al, EPAC08	Dean Adams, ISIS
6.	Injection Studies on the ISIS Synchrotron – B Jones et al, PAC07	Dean Adams, ISIS
7.	S.R. Johnson, W.I.F. David, D.M. Royle, M. Sommariva, C.Y. Tang, F.P.A. Fabbiani, M.O. Jones and P.P. Edwards, <i>Chem. Asian J.</i> , 2009, 4, 849-854	David Royle, ISIS
8.	Y.H. Guo, G.L. Xia, Y.H. Zhu, L. Gao, X.B. Yu, <i>Chem. Comm.</i> , 2010, 46 (15), 849-854	David Royle, ISIS
9.	C. H. Christensen, R. Z. Sørensen, T. Johannessen, U. J. Quaade, K Honkala, T. D. Elmøe, R. Köhler, J. K. Nørskov, <i>J. Mater. Chem.</i> , 2005, 15, 4106-4108	David Royle, ISIS
10.	Christine L. Bailey, Leandro Liborio, Giuseppe Mallia, Stanko Tomić, and Nicholas M. Harrison "Defect physics of CuGaS <sub>2</sub> " <i>Phys. Rev. B</i> 81, 205214 (2010)	Giuseppe Mallia, CSE
11.	Leandro M. Liborio, Christine L. Bailey, Giuseppe Mallia, Stanko Tomic, Nicholas M. Harrison "Chemistry of Defect Induced Photoluminescence in Chalcopyrites: The case of CuAlS <sub>2</sub> " submitted to "Journal of Applied Physics"	Giuseppe Mallia, CSE
12.	R. Martinez-Casado, G. Mallia, D. Usvyat, L. Maschio, S. Casassa, M. Schutz, and N. M. Harrison "Periodic quantum mechanical simulation of the He-MgO(100) interaction potential." submitted to "The Journal of Chemical Physics", under review	Giuseppe Mallia, CSE
13.	R. Kaur, G. Mallia, N. M. Harrison, "Computer Simulations of CrO <sub>2</sub> as a Spin Polarised Material for Spintronics", <i>TechConnect World 2010 Proceedings</i> , 2, 613 (2010).	Giuseppe Mallia, CSE
14.	I.J. Bush, S. Tomic, B.G. Searle, G. Mallia, C.L. Bailey, B. Montanari, L. Bernasconi, and N.M. Harrison "Parallel implementation of the ab initio CRYSTAL program: Electronic structure calculations for periodic systems" accepted in "Proc Roy Soc"	Giuseppe Mallia, CSE
15.	S Tomic, G Mallia, JM Carr, BG Searle, NM Harrison Massively Parallel CRYSTAL Calculations CSE Department's annual report for 2009 - entitled <i>Frontiers 2009</i>	Giuseppe Mallia, CSE
16.	"The solvent structure around n-Decyltrimethylammonium Bromide micelles" Rowan Hargreaves, Karen Edler and Daniel Bowron. In prep	Rowan Hargreaves, ISIS
17.	I. McKenzie, DFT Study of Paramagnetic Adducts of Tris-(8-hydroxyquinoline)aluminum(III), <i>J. Phys. Chem. A</i> , accepted	Iain McKenzie, ISIS
18.	I. McKenzie, Spin Relaxation of a Short-Lived Radical in Zero Magnetic Field, submitted to <i>Phys. Chem. Chem. Phys.</i>	Iain McKenzie, ISIS
19.	L. Schulz, M. Willis, L. Nuccio, P. Shusharov, S. Fratini, F. L. Pratt, W. Gillin, T. Kreouzis, M. Heeney, N. Stingelin, C. Stafford, D. Beesley, C. Bernhard, J.E. Anthony, I. McKenzie, J. S. Lord, A. J. Drew, Importance of intramolecular electron spin relaxation in small molecular semiconductors, submitted to <i>Phys. Rev. Lett.</i>	Iain McKenzie, ISIS
20.	Presentation: I. McKenzie, Muoniated Spin Probes in Soft Matter, ISIS High Field and User Meeting, September 6-7, 2010, Cosener's House, Abingdon, U.K.	Iain McKenzie, ISIS
21.	Presentation: I. McKenzie, Muoniated Spin Probes in Soft Matter, Simon Fraser University Department of Chemistry Seminar, October 12, 2010, Vancouver, B.C., Canada.	Iain McKenzie, ISIS
22.	Presentation: I. McKenzie, Muoniated Spin Probes in Soft Matter, University of British Columbia Department of Chemistry Seminar, November 2, 2010, Vancouver, B.C., Canada.	Iain McKenzie, ISIS
23.	Kideok D. Kwon, Keith Refson, and Garrison Sposito, <i>Geochimica Et Cosmochimica Acta</i> 73, 1273-1284 (2009).	Keith Refson, CSE
24.	Kideok D. Kwon, Keith Refson, and Garrison Sposito, <i>Geochimica Et Cosmochimica Acta</i> 73, 4142-4150 (2009). R. Gremaud, Z. Łodziana, P. Hug, B. Willenberg, A.-M. Racu, J. Schoenes, A. J. Ramirez-Cuesta, S. J. Clark, Keith Refson, Andreas Züttel, and A. Borgschulte, <i>Physical Review B</i> 80, 100301 (2009).	Keith Refson, CSE
25.	V. Milman, K. Refson, S.J. Clark, Christopher J Pickard, J.R. Yates, S.-P. Gao, P.J. Hasnip, M.I.J. Probert, A. Perlov, and M.D. Segall, <i>Journal Of Molecular Structure: THEOCHEM</i> (2010).	Keith Refson, CSE
26.	Pavlin D Mitev, Kersti Hermansson, Barbara Montanari, and Keith Refson, <i>Physical Review B</i> 81, 134303 (2010).	Keith Refson, CSE
27.	Stewart F. Parker, Daniel T. Bowron, Silvia Imberti, Alan K. Soper, Keith Refson, Egbert S. Lox, Marco Lopez, and Peter Albers, <i>Chemical Communications (Cambridge, England)</i> 46, 2959-61 (2010).	Keith Refson, CSE
28.	Jasquelin Peña, Kideok D. Kwon, Keith Refson, John R. Bargar, and Garrison Sposito,	Keith Refson, CSE

	Geochimica Et Cosmochimica Acta (2010).	
29.	Stewart F Parker, Keith Refson, Alex C Hannon, Emma R Barney, Stephen J Robertson, and Peter Albers, The Journal Of Physical Chemistry C 100804132703053 (2010).	Keith Refson, CSE
30.	Alexandra Friedrich, Björn Winkler, Lkhamsuren Bayarjargal, WolfgangMorgenroth, Erick Juarez-Arellano, Victor Milman, Keith Refson, Martin Kunz, and Kai Chen, Physical Review Letters 105, 1-4 (2010).	Keith Refson, CSE
31.	A Borgschulte, R Gremaud, K Refson, and A Züttel, Advances In Science And Technology 72, 150-157 (2010).	Keith Refson, CSE
32.	Stewart F. Parker, Keith Refson, Susan M Tavender, Peter Albers, Bernd Hannebauer, Matthias Janik, Arndt Mueller, Juergen Martens, Martin Watzke, Kenneth Shankland, Charlotte Leech, and Heribert Offermanns, JOURNAL OF RAMAN SPECTROSCOPY 40, 703-708 (2009).	Keith Refson, CSE
33.	Presentation: Sep "Structure and Dynamics of Hydrogen-Bonded Systems", ICTP Trieste "Strong Anharmonicity and Isotope Effects in CrOOH(D)" 02 Dec, Accelrys Webinar "Spectroscopic Modelling with CASTEP"	Keith Refson, CSE
34.	Presentation: 8 Feb 2010: Frankfurt Workshop "From atomistic simulations to thermodynamic modelling 2010": "Lattice Dynamics and Spectroscopy from DFT"	Keith Refson, CSE
35.	Presentation: 1 May 2010: MaMiNa workshop in Alloys in Edinburgh "Introduction to Computer Simulation of Alloys": "Concepts, Machinery and Codes"	Keith Refson, CSE
36.	Presentation: 7 May 2010 Materials Chemistry Consortium, UCL "New Developments in CASTEP"	Keith Refson, CSE
37.	Presentation: July 2010: CEA/LM2T, Saclay, Paris "Photocatalysis, vacancies and sorption in biogenic manganese dioxide"	Keith Refson, CSE
38.	Presentation: 24 June: Invitation to Juelich Forschungszentrum "Materials Modelling with CASTEP"	Keith Refson, CSE
39.	Presentation: 14 July: ISIS excitations user group meeting	Keith Refson, CSE
40.	Presentation: 12 Sep 2010: Psi-K 2010 Invited presentation "An ab-initio approach to experimental spectroscopy" 30 Sep 2010: BCS Fortran user meeting	Keith Refson, CSE
41.	Presentation: 30 Sep 2010: BCS Fortran user meeting "The CASTEP project: reflections on the first ten years"	Keith Refson, CSE
42.	Krzystyniak M, Lalowicz ZT, Chatzidimitriou-Dreismann CA, Lerch M, J. Phys. Condens. Matter, 21, 075502, (2009)	Matthew Krzystyniak, ISIS
43.	hydrogen bonding systems, liquid and solid hydrogen fluoride (HF) , Matthew Krzystyniak, J. Chem. Phys, in press (2010)	Matthew Krzystyniak, ISIS
44.	Calculations in hydrogen storage and proton conducting system, lithium hydride and lithium deuteride (LiH and LiD) [Matthew. Krzystyniak et al, Phys. Rev. B, in preparation	Matthew Krzystyniak, ISIS
45.	Yuan, X.H. et al., 2010. Effect of self-generated magnetic fields on fast-electron beam divergence in solid targets. New Journal of Physics, 12(6), 063018.	Mark Quinn, Strathclyde
46.	Quinn, M.N et al., 2010. Influence of low-temperature resistivity on fast electron beam filamentation in solid targets. (In preparation)	Mark Quinn, Strathclyde
47.	Quinn, M.N. et al., 2010. Refluxing of fast electrons in solid targets irradiated by intense , picosecond laser pulses. Plasma Physics and Controlled Fusion (Accepted).	Mark Quinn, Strathclyde
48.	M. N. Quinn, X. H. Yuan, D. C. Carroll, P. Gallegos, P. McKenna, A. P. L. Robinson, R. J. Clarke, D. Neely, R. G. Evans, L. Romagnani, K. Quinn, P. A. Wilson, G. Sarri, M. Borghesi, L. Lancia and J. Fuchs, 'Effects of scattering on fast electron transport in solid targets diagnosed via proton emission', Central Laser Facility Annual Report 2008-2009, P32	Mark Quinn, Strathclyde
49.	X. H. Yuan, M. N. Quinn, D. C. Carroll, P. Gallegos, P. McKenna, A. P. L. Robinson, R. J. Clarke, D. Neely,R. G. Evans, K. Quinn, L. Romagnani, G. Sarri, P. A. Wilson, M. Borghesi, L. Lancia and J. Fuchs, 'Magnetic pinching of fast electron transport in solid targets diagnosed using measurements of proton acceleration', Central Laser Facility Annual Report 2008-2009, P42	Mark Quinn, Strathclyde
50.	Presentation: "Investigations of fast electron generation and transport in dense plasma using the Vulcan PW laser", The 4th International Conference on Superstrong Fields in Plasmas, (2010)	Mark Quinn, Strathclyde
51.	Presentation: "Fast electron transport in dense plasma diagnosed via ion emission" The 14th International Conference on Laser-Optics, (2010)	Mark Quinn, Strathclyde
52.	Presentation: "Magnetic collimation and filamentation of fast electron transport in solid targets", Institute of	Mark Quinn, Strathclyde

	Physics Annual Plasma Physics Conference 2010, (2010)	
53.	Presentation: "Correlated diagnostics of fast electron transport in dense plasma", 1st International Workshop on Instrumentation for Diagnostics and Control of Laser-Accelerated Proton (Ion) Beams, (2010)	Mark Quinn, Strathclyde
54.	Presentation: "Laser-driven ion acceleration and nuclear physics at the ELI Nuclear Physics pillar", ELI Nuclear Physics Workshop, (2010)	Mark Quinn, Strathclyde
55.	Presentation: "Lateral fast electron transport and ion acceleration in thin foil targets irradiated by high intensity, picosecond laser pulses", European Physical Society, 37th Conference on Plasma Physics, (2010)	Mark Quinn, Strathclyde
56.	Presentation: "Progress in laser driven ion source development", LIBRA project Open Day, The Royal Society, (2010)	Mark Quinn, Strathclyde
57.	Presentation: "Magnetic collimation and filamentation of fast electron transport in solid targets", The 2nd International Conference on Ultra intense Laser Interaction Sciences, (2009)	Mark Quinn, Strathclyde
58.	Presentation: "Laser energy transfer to fast electrons in solid targets", PHELIX PPAC committee meeting, (2009)	Mark Quinn, Strathclyde
59.	Presentation: "Fast electron transport diagnosed by ion emission", HiPER project Diagnostics Workshop, Rutherford Appleton Laboratory, (2009)	Mark Quinn, Strathclyde
60.	C. L. Bailey, S. Mukhopadhyay, A. Wander, B. G. Searle and N. M. Harrison, "Reactivity of the beta-AlF <sub>3</sub> (100) surface: defects, fluorine mobility and catalysis of the CCl <sub>2</sub> F <sub>2</sub> dismutation reaction", <i>J. Phys. Chem. Chem. Phys.</i> 12, 6124 (2010).	Sanghamitra Mukhopadhyay, ICL, STFC
61.	S. Mukhopadhyay, M. W. Finnis and N. M. Harrison, "Electronic structure and phase stability of LaCoO <sub>3</sub> using Hybrid Exchange DFT ", Psik-2010 Conference, Berlin, Germany, held during 14-16th September (2010).	Sanghamitra Mukhopadhyay, ICL, STFC
62.	Presentation: S. Mukhopadhyay and N. M. Harrison, "Magnetic interaction in Mn doped dilute magnetic Silicon: an investigation using density functional theory.", Poster presentation, in International Symposium on Atom-Scale Silicon Hybrid Nanotechnologies for 'More-than-Moore' & 'Beyond CMOS' Era", University of Southampton, UK, held during 1 <sup>st</sup> - 2 <sup>nd</sup> March (2010).	Sanghamitra Mukhopadhyay, ICL, STFC
63.	Presentation: S. Mukhopadhyay, M. W. Finnis and N. M. Harrison, " Spin state and Electronic Transitions of LaCoO <sub>3</sub> ", Condensed Matter and Materials Physics Symposium (CMMP09), University of Warwick, UK, held during 14-16th December (2009).	Sanghamitra Mukhopadhyay, ICL, STFC
64.	[1]"Characterisation of hydrous palladium oxide: implications for low temperature carbon monoxide oxidation", S.F. Parker, K. Refson, A.C. Hannon, E. Barney, S.J. Robertson and P. Albers, <i>J. Phys. Chem. C</i> , 114 (2010) 14164-14172	Stewart Parker, ISIS
65.	[2]"Structure determination of adsorbed hydrogen on real catalysts", S.F. Parker, D.T. Bowron, S. Imberti, A.K. Soper, K. Refson, E.S. Lox, M. Lopez and P. Albers, <i>Chem. Comm.</i> 46 (2010) 2959 – 2961.	Stewart Parker, ISIS
66.	[3]"The reactions of iron atoms with benzene", S.F. Parker, <i>J. Phys. Chem. A</i> , 114 (2010) 1657-1664.	Stewart Parker, ISIS
67.	[4]"Vibrational spectroscopy of a compound with a C <sub>5</sub> ring", S.F. Parker, K. Refson, S.M. Tavender, P. Albers, B. Hannebauer, M. Janik, A. Müller, J. Martens, M. Watzke, K. Shankland, C. Leech and H. Offermanns, <i>J. Raman Spec.</i> , 40 (2009) 703-708.	Stewart Parker, ISIS
68.	[5]"Bonding and spectroscopy of LaMg <sub>2</sub> PdH: a compound with two types of hydride", S.F. Parker, J.W. Taylor, H. Herman, J.-P. Rapin, N. Penin and K. Yvon, <i>J. Alloys Compds.</i> , 470 (2009) 80-84.	Stewart Parker, ISIS
69.	Presentation: "Terahertz Spectroscopy with Neutrons", RSC Molecular Spectroscopy Group meeting on TeraHertz Spectroscopy (Cambridge, 28 <sup>th</sup> October 2009).	Stewart Parker, ISIS
70.	Presentation: "Vibrational Spectroscopy with Neutrons", BCA Chemical Crystallography meeting (Oxford, 18 <sup>th</sup> November 2009).	Stewart Parker, ISIS
71.	Borgschulte A, Zuttel A, Hug P, Barkhordarian G, Eigen N, Dornheim M, Bormann R, Ramirez-Cuesta A. Hydrogen-deuterium exchange experiments to probe the decomposition reaction of sodium alanate. <i>PHYSICAL CHEMISTRY CHEMICAL PHYSICS</i> 2008;10(27):4045-4055.	Timmy Ramirez-Cuesta, ISIS
72.	Bucher F, Lodziana Z, Mauron P, Remhof A, Friedrichs O, Borgschulte A, Zuttel A, Sheptyakov D, Strassle T, Ramirez-Cuesta A. Dynamical properties and temperature induced molecular disordering of LiBH <sub>4</sub> and LiBD <sub>4</sub> . <i>PHYSICAL REVIEW B</i> 2008;78(9)	Timmy Ramirez-Cuesta, ISIS

73.	Liu Y, Her J, Dailly A, Ramirez-Cuesta A, Neumann D, Brown C. Reversible structural transition in MIL-53 with large temperature hysteresis. JOURNAL OF THE AMERICAN CHEMICAL SOCIETY 2008;130(35):11813-11818.	Timmy Ramirez-Cuesta, ISIS
74.	Andresen E, Gremaud R, Borgschulte A, Ramirez-Cuesta A, Zuttel A, Hamm P. Vibrational Dynamics of LiBH <sub>4</sub> by Infrared Pump-Probe and 2D Spectroscopy. JOURNAL OF PHYSICAL CHEMISTRY A 2009;113(46):12838-12846.	Timmy Ramirez-Cuesta, ISIS
75.	Gremaud R, Lodziana Z, Hug P, Willenberg B, Racu A, Schoenes J, Ramirez-Cuesta A, Clark S, Refson K, Zuttel A, Borgschulte A. Evidence for hydrogen transport in deuterated LiBH <sub>4</sub> from low-temperature Raman-scattering measurements and first-principles calculations. PHYSICAL REVIEW B 2009;80(10)	Timmy Ramirez-Cuesta, ISIS
76.	Ramirez-Cuesta A, Jones M, David W. Neutron scattering and hydrogen storage. MATERIALS TODAY 2009;12(11):54-61.	Timmy Ramirez-Cuesta, ISIS
77.	Eblagon KM, Tam K, Yu KMK, Zhao SL, Gong XQ, He HY, Ye L, Wang LC, Ramirez-Cuesta AJ, Tsang SC. Study of Catalytic Sites on Ruthenium For Hydrogenation of N-ethylcarbazole: Implications of Hydrogen Storage via Reversible Catalytic Hydrogenation. Journal of Physical Chemistry C 2010;114(21):9720-9730.	Timmy Ramirez-Cuesta, ISIS
78.	Giannasi A, Colognesi D, Ulivi L, Zoppi M, Ramirez-Cuesta AJ, Bardaji EG, Roehm E, Fichtner M. High Resolution Raman and Neutron Investigation of Mg(BH <sub>4</sub> ) <sub>2</sub> in an Extensive Temperature Range. Journal of Physical Chemistry A 2010;114(8):2788-2793.	Timmy Ramirez-Cuesta, ISIS
79.	Mulder FM, Assfour B, Huot J, Dingemans TJ, Wagemaker M, Ramirez-Cuesta AJ. Hydrogen in the Metal-Organic Framework Cr MIL-53. Journal of Physical Chemistry C 2010;114(23):10648-10655.	Timmy Ramirez-Cuesta, ISIS
80.	Remhof A, Gremaud R, Buchter F, Lodziana Z, Embs JP, Ramirez-Cuesta TAJ, Borgschulte A, Zuttel A. Hydrogen Dynamics in Lightweight Tetrahydroborates. Zeitschrift Fur Physikalische Chemie-International Journal of Research in Physical Chemistry & Chemical Physics 2010;224(1-2):263-278.	Timmy Ramirez-Cuesta, ISIS
81.	Seel AG, Sartbaeva A, Ramirez-Cuesta AJ, Edwards PP. Inelastic neutron scattering of Na-zeolite A with in situ ammoniation: an examination of initial coordination. Physical Chemistry Chemical Physics 2010;12(33):9661-9666.	Timmy Ramirez-Cuesta, ISIS
82.	A. Borgschulte, R. Gremaud, A. J. Ramirez-Cuesta, K. Refson, A. Züttel. Evidence for Hydrogen Transport in Deuterated LiBH <sub>4</sub> from Raman-scattering Measurements and First-principles Calculations. Advances in Science and Technology Vol. 72 (2010) pp 150-157	Timmy Ramirez-Cuesta, ISIS
83.	Eblagon KM, Rentsch D, Friedrichs O, Remhof A, Zuttel A, Ramirez-Cuesta A, Tsang SC. Hydrogenation of 9-ethylcarbazole as a prototype of a liquid hydrogen carrier. International Journal of Hydrogen Energy 2010 Oct;35(20):11609-116211.	Timmy Ramirez-Cuesta, ISIS
84.	Sartbaeva A, Wells S, Sommariva M, Lodge M, Jones M, Ramirez-Cuesta A, Li G, Edwards P. Formation of Crystalline Sodium Hydride Nanoparticles Encapsulated Within an Amorphous Framework. Journal of Cluster Science 2010 Sep;21(3):543-549.	Timmy Ramirez-Cuesta, ISIS
85.	Presentation: SPAIN: 4th Meeting of the Spanish Neutron Society, Sant Felieu de Guixols, Spain (September 2008)	Timmy Ramirez-Cuesta, ISIS
86.	Presentation: UK: UK-Korea Hydrogen Storage Meeting, University of Birmingham (October 2008)	Timmy Ramirez-Cuesta, ISIS
87.	Presentation: UK: Inorganic Chemistry Laboratory, University of Oxford (September 2008)	Timmy Ramirez-Cuesta, ISIS
88.	Presentation: USA: ISIS Crystallography Users Group Meeting, Abingdon (November 2008)	Timmy Ramirez-Cuesta, ISIS
89.	Presentation: SWITZERLAND: 3rd Symposium Hydrogen and Energy in Braunschwald Switzerland (January 2009).	Timmy Ramirez-Cuesta, ISIS
90.	Presentation: USA: 'Studying the Interaction of Molecular Hydrogen with Surfaces using Inelastic Neutron Scattering,' International Conference on Neutron Scattering ICNS 2009, Knoxville, May 2009	Timmy Ramirez-Cuesta, ISIS
91.	Presentation: JAPAN: 'Di-hydrogen in Porous Materials & Surfaces, Probing the Interactions of Hydrogen Molecules with the Host Material: Timmy Ramirez-Cuesta, ISIS Characterization of the Interaction strength,' 4th UK - Japan Workshop on Solid-State Hydrogen Storage, Tohoku University, Sendai, May 2009	Timmy Ramirez-Cuesta, ISIS
92.	Presentation: ITALY: Gordon Conference in Hydrogen Storage in Lucca, Italy (July 2009).	Timmy Ramirez-Cuesta, ISIS
93.	Presentation: USA: 'Using Inelastic Neutron Scattering to Elucidate Mechanisms in Hydrogen Storage Materials,' Fundamental and Computational Sciences Directorate, Pacific Northwest National	Timmy Ramirez-Cuesta, ISIS

SCARF Annual Report 2009-2010 v1.2

	Laboratory, Richland, Washington State, August 2009	
94.	Presentation: USA: 'Ab Initio Calculations of the Dynamics of Some Hydrogen Storage Materials: Comparing Inelastic Neutron Scattering Spectra,' Fall 2009 Meeting of the American Chemical Society, Washington DC, August 2009	Timmy Ramirez-Cuesta, ISIS
95.	Presentation: SWITZERLAND: 4th International Conference on Hydrogen & Energy from 24 – 29 January 2010, Wildhaus, Switzerland.	Timmy Ramirez-Cuesta, ISIS
96.	Presentation: USA: 'Spectroscopic insights in the chemistry of Ammonia Borane and derivatives' IPHE meeting (International Partnership on Hydrogen Energy, Richland, Pacific Northwest National Laboratory, Richland, Washington State, April 2010.	Timmy Ramirez-Cuesta, ISIS
97.	Presentation: SWITZERLAND 'Inelastic Neutron Scattering for the study of hydrogen adsorption on porous solids', Gas separation and gas storage using porous materials Lausanne, 17-19 May, 2010	Timmy Ramirez-Cuesta, ISIS
98.	Presentation: USA 'The Power of Inelastic Neutron Scattering', Neutrons for Catalysis: A Workshop on Neutron Scattering Techniques for Studies in Catalysis, Oak Ridge National Laboratory, Oak Ridge, TN, USA, September 16-17, 2010.	Timmy Ramirez-Cuesta, ISIS
99.	Presentation: IRELAND 'Ab-Initio Calculations Of The Dynamics Of Select Hydrogen Storage Materials, Compared To Inelastic Neutron Scattering Spectra', Dublin, October 11-13, 2010.	Timmy Ramirez-Cuesta, ISIS
100.	A.P.L.Robinson, P.Gibbon, M.Zepf, S.Kar, R.G.Evans, C.Bellei, Plasma Phys. Control. Fusion, 51 , 024004 (2009)	CLF Plasma Physics
101.	A.P.L.Robinson, P.Gibbon, S.M.Pfotenhauer, O.Jaeckel, J.Polz, Plasma Phys. Control. Fusion, 51,	CLF Plasma Physics
102.	A.P.L.Robinson, D-H Kwon, and K.L.Lancaster, Plasma Phys. Control. Fusion 51 095006 (2009)	CLF Plasma Physics
103.	A.P.L.Robinson, P.Foster, D.Adams, et al., New J.Phys., 11, 083018 (2009)	CLF Plasma Physics
104.	S.Kar, A.P.L.Robinson, et al., Phys. Rev. Lett., 102, 055001 (2009)	CLF Plasma Physics
105.	S.Mondal et al., Phys.Rev.Lett.,105, 105002 (2010)	CLF Plasma Physics
106.	F.Zamponi et al., Phys.Rev.Lett., 105, 085001 (2010)	CLF Plasma Physics
107.	X.H.Yuan, A.P.L.Robinson et al., New J.Phys., 12, 063018 (2010)	CLF Plasma Physics
108.	D.C. Carroll et al., New J.Phys., 12, 045020 (2010)	CLF Plasma Physics
109.	B.Ramakrishna, S.Kar, A.P.L.Robinson et al., Phys.Rev.Lett., 105, 135001 (2010)	CLF Plasma Physics
110.	R. Trines, F. Fiuza, R. Bingham, R. Fonseca, L.O. Silva, A. Cairns and P. Norreys "Simulations of efficient Raman amplification into the multi-Petawatt regime" Nature Physics, PUBLISHED ONLINE: 10 OCTOBER 2010   DOI: 10.1038/NPHYS1793	CLF Plasma Physics
111.	R M G M Trines, R Bingham, Z Najmudin, S Mangles, L O Silva, R Fonseca and P A Norreys "Electron trapping and acceleration on a downward density ramp: a two-stage approach" New Journal of Physics 12, 045027 (2010)	CLF Plasma Physics
112.	G. Sarri, K. Lancaster, R. Trines, et al., "Creation of persistent, straight, 2mm long laser driven channels in underdense plasmas" Physics of Plasmas, in press (2010)	CLF Plasma Physics
113.	A.P.L.Robinson, P.Gibbon, M.Zepf, S.Kar, R.G.Evans, C.Bellei, Plasma Phys. Control. Fusion, 51 , 024004 (2009)	CLF Plasma Physics
114.	A.P.L.Robinson, P.Gibbon, S.M.Pfotenhauer, O.Jaeckel, J.Polz, Plasma Phys. Control. Fusion, 51,	CLF Plasma Physics
115.	A.P.L.Robinson, D-H Kwon, and K.L.Lancaster, Plasma Phys. Control. Fusion 51 095006 (2009)	CLF Plasma Physics
116.	A.P.L.Robinson, P.Foster, D.Adams, et al., New J.Phys., 11, 083018 (2009)	CLF Plasma Physics
117.	S.Kar, A.P.L.Robinson, et al., Phys. Rev. Lett., 102, 055001 (2009)	CLF Plasma Physics
118.	S.Mondal et al., Phys.Rev.Lett.,105, 105002 (2010)	CLF Plasma Physics
119.	F.Zamponi et al., Phys.Rev.Lett., 105, 085001 (2010)	CLF Plasma Physics
120.	T.Baeva, A.P.L.Robinson, S.Gordienko, P.A.Norreys, arXiv:1009.0848 (in prep)	CLF Plasma Physics
121.	A.P.L.Robinson – Work on Fast Electron Guiding for Fast Ignition ICF (in prep)	CLF Plasma Physics
122.	A.P.L.Robinson – Work on new scheme for RPA of ions (in prep)	CLF Plasma Physics
123.	A.P.L.Robinson – Paper under review by New J.Phys. (in prep)	CLF Plasma Physics
124.	R.M.G.M. Trines, P.A. Norreys, R.A. Fonseca, L.O. Silva, C. Kamperidis, K. Krushelnick and Z. Najmudin "Effect of channel profile evolution on laser-driven electron acceleration in plasma channels"	CLF Plasma Physics
125.	CLF Annual Report 2009-10, in press (2010).	CLF Plasma Physics
126.	CLF Annual Report 2008-09	CLF Plasma Physics
127.	Presentation: Alex Robinson, Contributed, American Physical Society Division of Plasma Physics Annual Meeting 2009 "Radiation Pressure Acceleration"	CLF Plasma Physics
128.	Presentation:	CLF Plasma Physics

	Alex Robinson, Invited, International Congress on Plasma Physics, 8th-13th August 2010 "Radiation Pressure Acceleration: Early Results and Forward Look"	
129.	Presentation: Alex Robinson, Invited, Fusion Science Centre Special Meeting on Electron Divergence, 4th-6th August 2010 "Guiding and Collimating Fast Electrons using Resistivity Gradients"	CLF Plasma Physics
130.	Presentation: Alex Robinson, Invited, EMMI workshop on Charged Particle Dynamics 2010 "Assembly of targets for RPA using Compression Waves"	CLF Plasma Physics
131.	Presentation: Alex Robinson, Invited, Trans-Regio 18 2010 "Assembly of targets for RPA using Compression Waves"	CLF Plasma Physics
132.	Alex Robinson, Contributed, IOP Plasma Physics, 2009	CLF Plasma Physics
133.	Alex Robinson, Contributed, IOP Plasma Physics, 2010	CLF Plasma Physics
134.	Alex Robinson, Contributed, Plasma: Mathematics, Computation and Theory, 2009	CLF Plasma Physics
135.	Robbie Scott, Contributed, IOP Plasma Physics 2010 Robbie Scott, Contributed, Direct drive and fast ignition workshop 2010	CLF Plasma Physics
136.	R. Trines, P. Norreys "Electron trapping and acceleration on a downward density ramp: a two-stage approach" 36th IoP Conference on Plasma Physics, Warwick University, Coventry, April 2009	CLF Plasma Physics
137.	R. Trines, F. Fiuza, Bingham, R. Fonseca, L.O. Silva, A. Cairns and P. Norreys "Numerical studies of nonlinear Raman amplification of laser pulses in plasma" 36th IoP Conference on Plasma Physics, Warwick University, Coventry, April 2009	CLF Plasma Physics
138.	R. Trines, P. Norreys "Electron trapping and acceleration on a downward density ramp: a two-stage approach" Laser and Plasma Accelerators Workshop 2009, Kardamily, Greece, June 2009	CLF Plasma Physics
139.	R. Trines, P. Norreys "Electron trapping and acceleration on a downward density ramp: a two-stage approach" Plasmas, Computation and Mathematics Workshop, Ambleside, Cumbria, July 2009	CLF Plasma Physics
140.	R. Trines, P. Norreys, G. Sarri, M. Borghesi "Numerical simulations of laser hole boring for fast ignition fusion" 51st Annual Meeting of the APS Division of Plasma Physics, Atlanta, GA, USA, November 2009	CLF Plasma Physics
141.	R. Trines, P. Norreys, G. Sarri, M. Borghesi "Numerical simulations of laser hole boring for fast ignition fusion" CLF Christmas Meeting of the High Power Laser Science Community 2009	CLF Plasma Physics
142.	R. Trines, F. Fiuza, R. Bingham, R. Fonseca, L.O. Silva, A. Cairns and P. Norreys "Efficient Raman amplification into the multi-Petawatt regime" 37th IoP Conference on Plasma Physics, Windermere, Cumbria, April 2010	CLF Plasma Physics
143.	R. Trines, F. Fiuza, R. Bingham, R. Fonseca, L.O. Silva, A. Cairns and P. Norreys "Simulations of efficient Raman amplification into the multi-Petawatt regime" International Advanced Workshop on the Frontiers of Plasma Physics Abdus Salam ICTP, Trieste, Italy, July 2010	CLF Plasma Physics
144.	R. Trines, F. Fiuza, R. Bingham, R. Fonseca, L.O. Silva, A. Cairns and P. Norreys "Simulations of efficient Raman amplification into the multi-Petawatt regime" 52nd Annual Meeting of the APS Division of Plasma Physics, Chicago, IL, USA, November 2010	CLF Plasma Physics
145.	1st International Particle Accelerators Conference (IPAC'10), Kyoto, Japan, 24-28 May 2010	Stephen Brooks, AsTeC
146.	C. W. Yong, C. Washington and W. Smith, 'Structural Behaviour of 2hydroxypropyl-b-cyclodextrin in water: Molecular dynamics simulation studies', Pharm. Res. vol.25 p1092 (2008)	Chin Young, CSE
147.	C. W. Yong, et. al., 'Assessment of long-term molecular dynamics calculations with experimental information on protein shape from X-ray scattering - SOD1 as a case study', Chem. Phys. Lett. Vol. 481 p112 (2009)	Chin Young, CSE
148.	C. W. Yong, R. W. Strange, S. S. Hasnain 'Molecular dynamics simulations reveal monomerisation of human wild-type Cu, Zn superoxide dismutase dimer: Investigation of the dimeric interface interaction', manuscript in preparation.	Chin Young, CSE

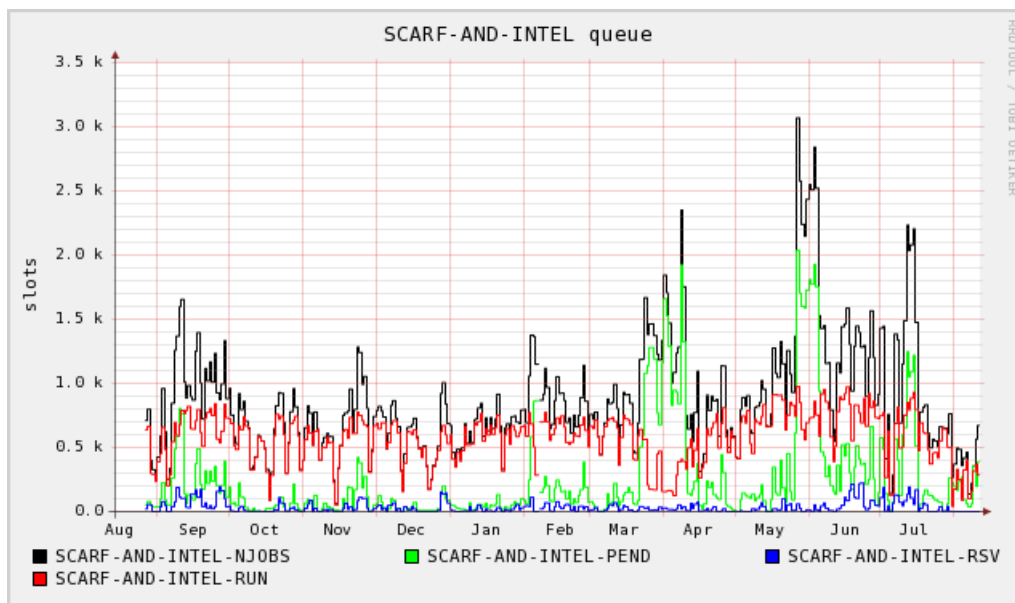
#### 4. APPENDIX: SCARF QUEUE USAGE 2009-10

Key:

- Red - number of jobs running
- Green - number of jobs pending
- Blue - number of jobs gather CPUs so that they can run (large parallel jobs)
- Black - total number of Jobs (sum of Red, Green, Blue)

##### 4.1 General SCARF Queue

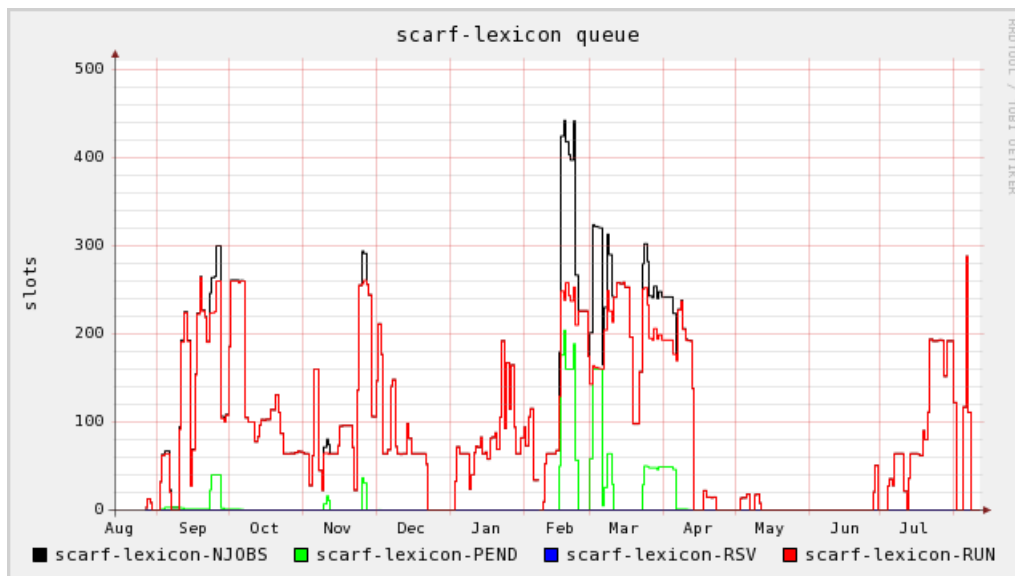
Open to all SCARF Users with a capacity of ~1080 CPU cores



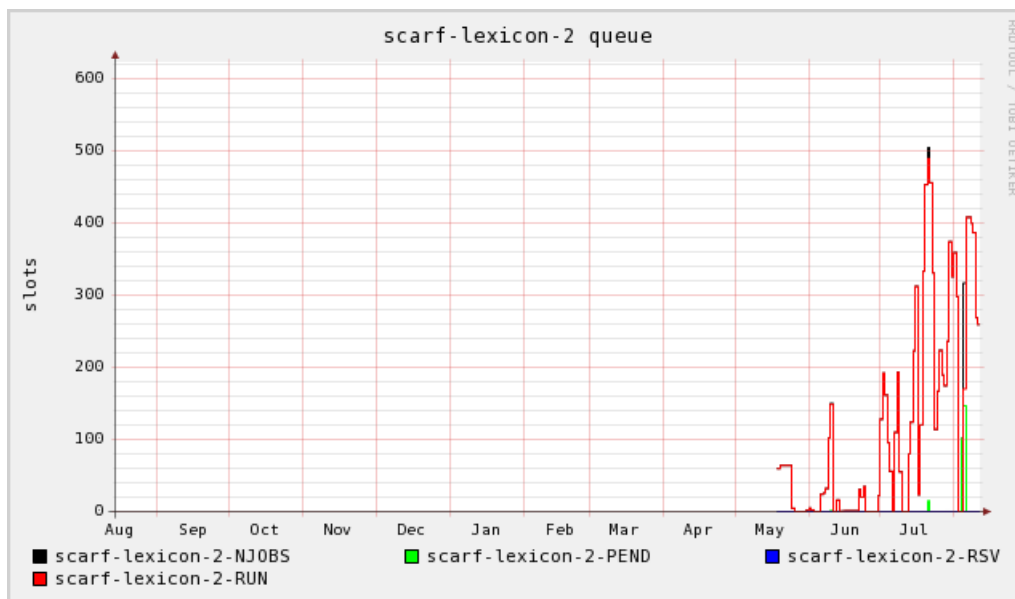
The graph for the SCARF queue (and thus the combined SCARF/INTEL graph) shows consistently pending jobs for most of the year, which demonstrates that there is not sufficient capacity. This should be addressed by the next hardware procurement.

## 4.2 SCARF-Lexicon[1-2] Queues

These queues is primarily for CLF use with a capacity of 292 and 544 CPU cores for SCARF Lexicon 1 & 2 respectively.



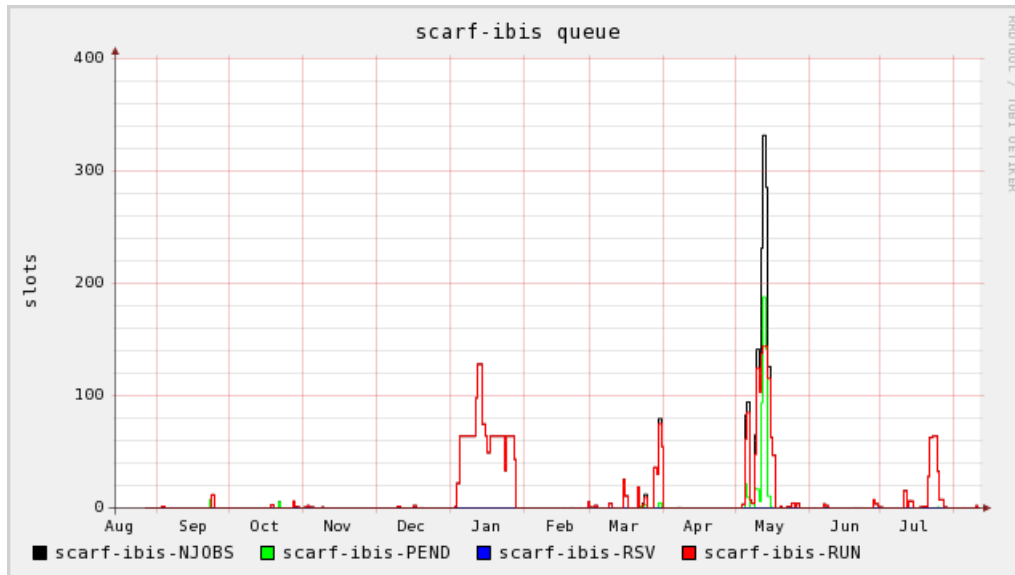
The graph for the SCARF-LEXICON queue shows peaky but significant usage, though this has dropped somewhat since the purchase of SCARF-LEXICON-2.



SCARF-LEXICON-2 shows steadily increasing usage towards the maximum capacity, which is excellent given that there have been some initial issues with the hardware which have reduced the amount of time available to the group.

### 4.3 SCARF-IBIS

SCARF-IBIS has a capacity of 144 CPU cores.



## 5. APPENDIX – SCARF DEVELOPMENTS

It has been a busy year for the SCARF service. Users' will have noticed most impact with the additional of capacity, upgrades to applications and a change in access to SCARF. However, a lot of effort goes into improving the management of SCARF. SCARF is also part of NGS which allows users to use grid technology to access a larger pool of resources.

### 5.1 NGS Software Stack

Support of the NGS Software Stack and conformance to NGS Affiliate Status.

- User Interface/Workload Management System (UI/WMS ) support
- New Globus Grid gateway with NGS accounting support
- Start of taster jobs up to 6 hours to NGS users. Trials back-filling SCARF capacity to maximise return on investment for UK science.
- Formation of scarf.rl.ac.uk Virtual Organisation (VO ) to better support remote users familiar with Grid and gLite technologies.

### 5.2 SCARF Systems Management

To ensure that SCARF continues to deliver excellent value to users process and procedures are continually being reviewed and updated.

- Seamless migration of head node to a virtual machine. Allowing service resilience and instantly upgradeable memory and CPU.
- SCARF attained and overall top score in the e-Science Centre's review of services. This covers aspects such as Service Overview, Service Levels, Data Integrity, Operations, Security, Monitoring, Reporting and Dependencies. This ensures that SCARF remains well managed and all services within the e-Science Centre can take advantage Best Practice.
- Started work on a web services interface to the cluster.
- Started work on migration to LSF v7, Platform MPI8 and RHEL5
- Temperature monitoring, Cabling Database, Remote Power Management, IPMI infrastructure.
- Replacement of Commercial OS deployment tool with in house technology – saved budget and now OS deployment meets our exact needs.
- Continued working in a challenging R89 Machine room environment caused by high levels of dust requiring facemasks in addition to the eardefenders.

### 5.3 People

There was a change of management of the SCARF service as Duncan Tooke left STFC for another role with MRC. Jonathan Churchill has taken over managing SCARF.

There has been a high turnover of staff in the e-Science Centre. This combined with STFC's restrictions on recruitment meant we did less development than in previous years. However, SCARF remains a strategic priority for the e-Science Centre and continues to be supported.